DECOUPLING OF CARBON AND URANIUM ISOTOPE ANOMALIES IN NEOPROTEROZOIC CARBONATES

MATT PEDERSEN
ADVISOR: DR. ALAN JAY KAUFMAN
CO-ADVISORS: GEOFFREY J. GILLEAUDEAU, TIAN GAN

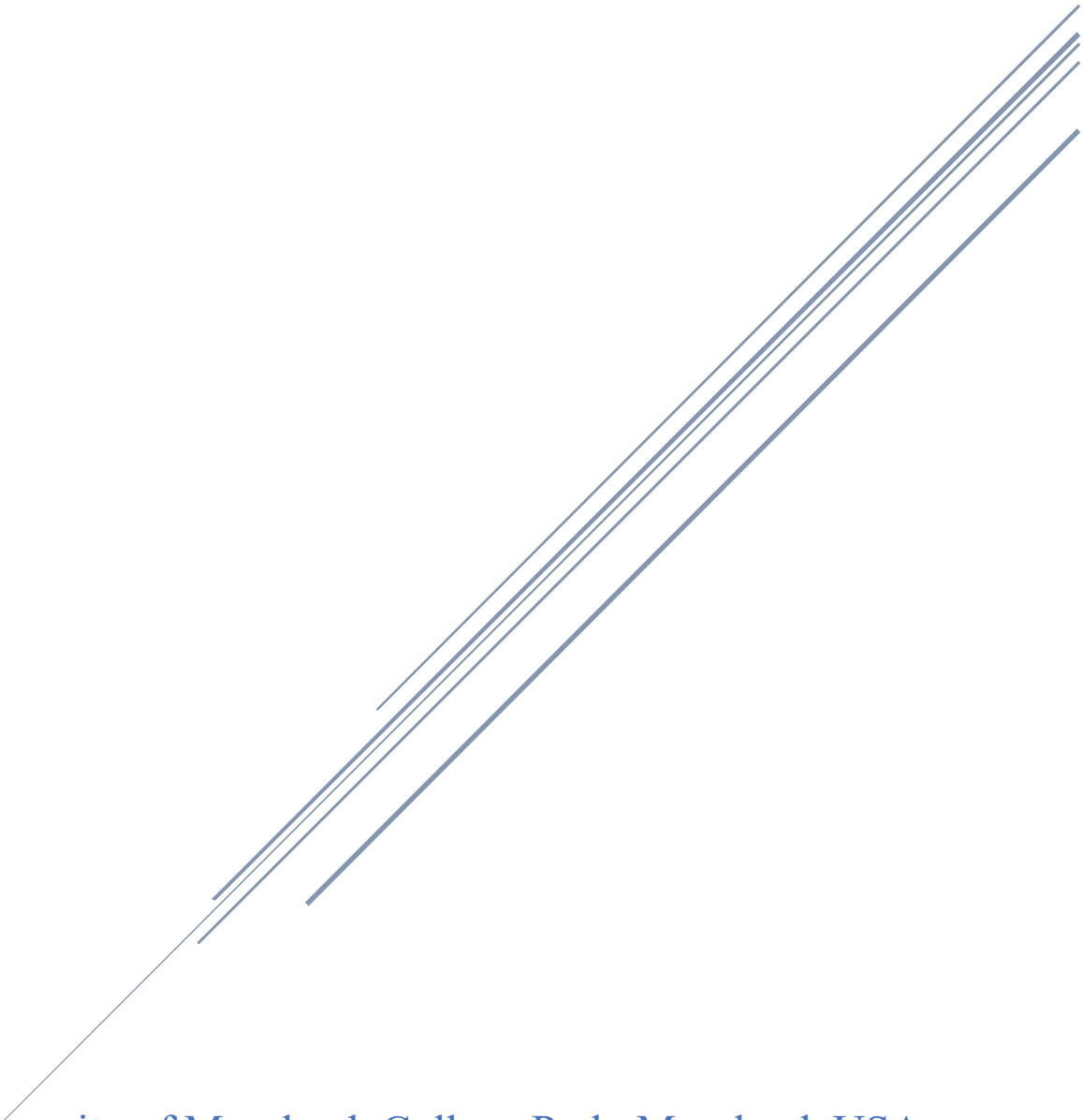

University of Maryland, College Park, Maryland, USA
GEOL394

Abstract

Proxy studies of Neoproterozoic carbonates suggest that strong positive $\delta^{13}C$ anomalies tend to preserve significant deviations to more negative $\delta^{238}U$ values, which likely reflect expanded euxinic conditions in the global oceans. Conversely, carbonates of this era that preserve profound negative $\delta^{13}C$ trends are characterized by $\delta^{238}U$ enrichment, suggesting oxic or ventilated conditions. The Siberian carbonate successions in this study accumulated in the late Cryogenian to middle Ediacaran periods (ca. 650-550 Ma). The younger formation, the Chencha, is exposed in the Patom/Ura Uplift and preserves a strong negative $\delta^{13}C$ anomaly attributed to the Shuram Excursion, one of the greatest carbon cycle perturbations in Earth history. The other formation is the Chernaya Rechka, located south of Igarka on the Igarka Uplift. This succession is associated with a strong positive $\delta^{13}C$ excursion that occurred either before or after the Marinoan glaciation. To better understand redox in the global ocean and the depositional basins during both biogeochemical events, the analysis of uranium isotope abundances was employed. The uranium isotopes are reflective of global redox due to the element's long half-life, meaning it is uniformly distributed throughout the world's oceans. The results thus far are consistent with the hypothesis that more positive $\delta^{13}C$ is associated with more negative $\delta^{238}U$, meaning that the oceans during the terminal Cryogenian underwent a period of expanded ocean euxinia while during the middle Ediacaran, during the enigmatic Shuram Excursion and immediately after, the oceans were more ventilated and oxygenated.

Plain Text Abstract

Insofar as animals need oxygen to breathe, geobiologists have sought for geochemical benchmarks that provide measures of the oxidation state of seawater during the rise of multicellular organisms on Earth. In this study, I have used carbon and uranium isotope abundances in marine carbonates to evaluate oceanic oxygen levels in the Ediacaran (ca. 635-538.8 million years ago) and Cryogenian (ca. 720-635 million years ago) periods when the earliest animals arose. Both studied successions are from the Siberian Craton, with one, the Chencha Formation, dating to 564 ± 24 million years while the other, the Chernaya Rechka Formation, dates to 610 ± 50 million years. In the younger example, we find depletion in the heavy isotope of carbon, but an enrichment of the heavy isotope of uranium, which suggests greater degrees of ocean oxygenation, while the opposite is true in the older example, suggesting that seawater was lacking in oxygen at that time. The decoupling of carbon and uranium systems appears to be consistent throughout the late Precambrian and Phanerozoic, providing a link between the evolution of animals and the rise and fall of oxygen at a critical time in Earth history.

Table of Contents

Introduction

The Neoproterozoic oceans were characterized by periods of widespread euxinia (Lau et al., 2017; Zhang et al., 2018; Cherry et al., 2022), as well as intervals of enhanced oxic (or ventilated) conditions (Canfield et al., 2007; Sahoo et al., 2016; Zhang et al., 2019). Carbonates that accumulated at these times may reflect these environments through their stable carbon isotope compositions. Variations in $\delta^{13}C$ compositions of carbonates may reflect time-averaged changes in the organic carbon (OC) burial flux insofar as photosynthetically produced organic matter is highly depleted in ^{13}C (Broecker, 1970; Hayes, 1983). During periods of widespread euxinia, it is likely that more organic matter would be preserved in ocean sediments leaving the pool of dissolved carbon (available for subsequently formed carbonate minerals) enriched in ^{13}C ($+\delta^{13}C$ values) (Lau et al., 2017). In contrast, periods of ocean oxygenation would increase aerobic respiration rates and decrease the flux of organic matter to sediments, leading to greater enrichments of ^{12}C ($-\delta^{13}C$ values) in subsequently formed carbonates.

Terminal Ediacaran carbonates across the globe preserve one of the largest negative $\delta^{13}C$ excursions in Earth history (indicated by the red star in Fig. 1), referred to as the Shuram Excursion (Grotzinger et al., 2011; Zhang et al., 2019). Named after the Shuram Formation in Oman, where it was first recognized, the carbon cycle anomaly has been a source of intense debate due to the absence of a reliable chronology, as well as the degree of ^{13}C depletion, and potential for diagenetic alteration in such ancient carbonate deposits. While several studies suggest the termination of the Shuram Excursion was around 550 Ma (e.g., Condon et al., 2005), recent Re-Os dating of black shales from Oman have constrained the onset of the Shuram Excursion to 574.0 ± 4.7 Ma and its termination around 567.3 ± 3.0 Ma (Rooney et. al., 2020). This date places the Shuram Excursion roughly 5 Ma after the Gaskiers glaciation (Pu et al., 2016), which is preserved as a diamictite in Newfoundland.

What makes the Shuram so intriguing is why the carbon cycle anomaly reaches such negative extremes. The profound biogeochemical event, which has been considered to be an ocean alkalinity anomaly, is preserved in a wide range of carbonate lithofacies on multiple continents, so it is arguably a palaeoceanographic event. However, since the mantle input to surface environments has a value of -6‰, some additional source of alkalinity depleted in ^{13}C is required to generate global values as low as -12‰ (Blank et al., 1993). For this reason, some have considered this globally-distributed anomaly to be of diagenetic origin (e.g. Knauth and Kennedy, 2009; Derry, 2010), who base the majority of their argument on the covariation of carbon and

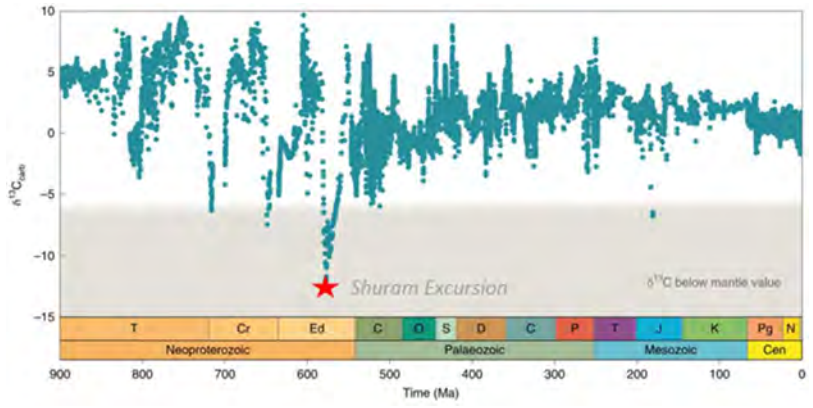

Figure 1: $\delta^{13}C$ values from the rise of the Neoproterozoic to the modern day. Values of ~-12‰ in the middle Ediacaran correspond to the Shuram Excursion. The values appear to constantly fluctuate rather than remain positive or negative for an extended period of time. During the periods of enhanced oxidation, it is hypothesized that Ediacaran biota were the most abundant (modified after Shields et al., 2019).

oxygen isotope values. In the papers, they explain the breakdown and oxidation of plants would lead to alkalinity that is depleted in ^{13}C. By combining this depleted alkalinity with freshwater, which is depleted in ^{18}O, water flowing through carbonates would lower isotopic values, therefore altering any pre-existing carbonates. Others such as Rothman et al. (2003) consider it to reflect disequilibrium in the world's oceans with pre-Shuram conditions characterized by anoxic oceans containing a high percentage of dissolved organic carbon (DOC), which was subsequently oxidized to dissolved carbonate ions (requiring anaerobic processing) resulting in the strongly negative $\delta^{13}C$ values of Shuram carbonates.

Shortly after the onset of the Shuram Excursion there was also a rise in multicellular organisms that would populate the rest of the Ediacaran Period. The new discoveries of *Cloudina*, the early worm-like metazoan with a carbonate shell in the Mara Member of the Nama Group in southern Namibia (a recognized Shuram equivalent), and of sponge-grade organisms preserved as bioclasts in the Chencha Formation (another Shuram equivalent) reef complex are of particular interest in the study of oceanic redox conditions at this time. The Shuram Excursion and the rise of Ediacaran biota appear to be coupled in some way as the enigmatic event is reflected in carbonates that also preserve body fossils belonging to multicellular organisms. Understanding the redox conditions of the Neoproterozoic oceans provide insight into the natural processes that drive the carbon cycle to negative or positive extremes. Additionally, ventilation of the oceans during the Shuram Excursion might explain the diversification of animals in its aftermath insofar as they need oxygen to respire and make a living.

The extreme positive and negative $\delta^{13}C$ values preserved in Neoproterozoic carbonates suggest the carbon cycle was drastically different compared to the modern carbon cycle. This study focuses on two formations both located on the Siberian Craton. One formation, the reef complex of the Chencha Formation from the Patom/Ura Uplift, preserves a strong negative $\delta^{13}C$ anomaly while the other formation, the Chernaya Rechka, preserves a strong positive $\delta^{13}C$ anomaly.

Systematics of geochemical tests for global euxinia

Carbon isotopes

Carbon isotope data ($\delta^{13}C$) is critical in reconstructing secular shifts in the composition of seawater throughout Earth history, correlating between stratigraphic intervals locally and globally, and constructing chemostratigraphic age models (Nelson et al., 2021; Saltzman and Thomas 2012). $\delta^{13}C$ and $\delta^{18}O$ values of carbonate rocks are reflective of dissolved inorganic carbon (DIC) in seawater which may be shifted by the effects of diagenetic and metamorphic

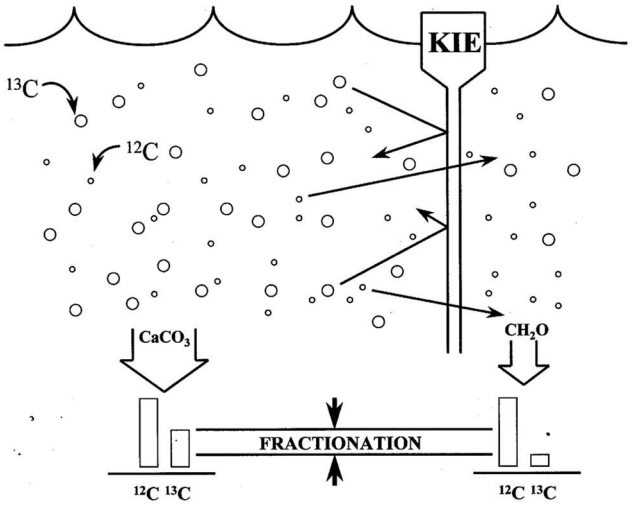

Figure 2: Schematic illustrating the fractionation of carbon in seawater between carbonate carbon ($CaCO_3$) and organic matter (abbreviated as CH_2O).

alteration. There are two primary processes of drawing carbon out of seawater: the formation of carbonates and organic matter (Fig. 2). Carbonates will take ^{12}C and ^{13}C in the same proportion as seawater. On the other hand, in the autotrophic fixation of CO_2, ^{12}C is preferentially incorporated relative to ^{13}C determined by the kinetic properties of the CO_2-fixing enzyme and the availability of CO_2 at the molecular site of fixation. Photosynthetic uptake of the isotopically light ^{12}C leaves the DIC of the surface ocean enriched in the isotopically heavy ^{13}C (Kaufman and Knoll, 1995). The difference in isotopic composition of carbonate and organic carbon is measured as a fractionation. Under periods of expanded euxinia, there is enhanced organic carbon burial, stimulated by an increase in primary productivity, resulting in seawater that is enriched in the heavier isotope that are reflected in any carbonates that formed subsequently. Under more oxic (or ventilated) conditions, dissolved organic matter depleted in ^{13}C may be converted to alkalinity, which results in the formation of carbonates with negative $\delta^{13}C$ values.

Uranium isotopes

To investigate seawater redox conditions uranium is used as a global indicator. $\delta^{238}U$ values reflect the abundance of the isotopically heavy and more abundant ^{238}U and the isotopically light and less abundant ^{235}U. In the modern ocean, uranium has a concentration of roughly 3.2 ppb and a residence time of approximately 500 kyr. The typical thermohaline cycle in the ocean is approximately 1 kyr meaning $\delta^{238}U$ values are very uniform in an oxidized open ocean (Zhang et al., 2018). Additionally, uranium exists in two natural redox states, the soluble U(VI) which is responsible for forming calcium-uranyl-bicarbonate structures under oxidized conditions. Under euxinic conditions, U(VI) is reduced to the insoluble U(IV), a redox state that preferentially sequesters the ^{238}U isotope leaving a reservoir depleted in the heavier isotope and enriched in the lighter isotope (Cherry et al., 2022). Among the various sinks for seawater, euxinic sediments are by far the largest (Fig. 3). Uranium-238 is preferentially sequestered in euxinic sediments, meaning it also reflects the strongest isotopic fractionation compared to the various other sinks. Carbonate sediments are the second largest sink for seawater uranium. However, because the euxinic sediments pull the heavier ^{238}U from the reservoir, the carbonate sediments become enriched in the lighter ^{235}U which is reflected by a strong negative $\delta^{238}U$ composition (Stirling et al., 2015, Lau et al., 2017).

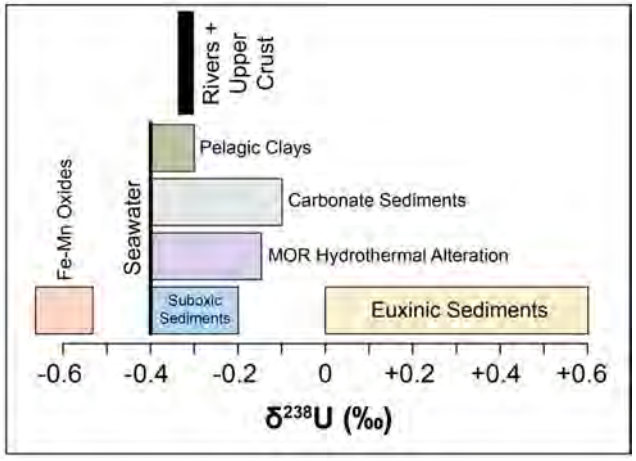

Figure 3: Mass balance model for the various sinks for seawater $\delta^{238}U$. Euxinic sediments represent the largest sink for uranium. The other sinks are carbonates, mid-ocean ridge hydrothermal alteration, suboxic sediments, pelagic clays, and Fe-Mn Oxides (after Tissot and Dauphas, 2015).

Rare Earth Elements

To investigate local redox conditions of the overlying water column, the analysis of Rare Earth Elements (REEs) is employed. One element, cerium, is unique amongst the other REE because it can exist in both the +3 and +4 oxidation state. Under oxic conditions, Ce(III) is partially oxidized to Ce(IV) on the surface of Mn oxides, where it no longer participates in solid-solution exchange reactions, leaving the residual seawater depleted in Ce relative to the other REE (Tostevin et al., 2016). Cerium anomalies are calculated by comparing the normalized concentrations of Ce to its neighboring REE using the following equation:

$$\frac{Ce_{SN}}{Ce^*_{SN}} = \frac{[Ce]_{SN}}{(\frac{[Pr]^2_{SN}}{[Nd]_{SN}})}$$

Negative Ce anomalies are pervasive in the modern, well-oxygenated ocean, but their magnitude varies within and between ocean basins (De Baar et al., 1985a, De Baar, 1991, Tostevin et al., 2016), and can respond to changes in water column redox on a meter scale (De Carlo and Green, 2002). Under anoxic conditions, Ce remains in the Ce(III) state and is not removed from the water column which results in a Ce/Ce* ratio that is greater than or equal to 1. In addition to Ce anomalies, yttrium to holmium (Y/Ho) ratios can be used to screen for detrital influence within the samples with values >36 indicating an authigenic seawater signal (Cherry et al., 2022). Combining the U analysis with REE analysis, the comprehensive profile of both local and global redox conditions during the depositional period of these two formations provides insight into whether the carbon and uranium systems were coupled during the late Neoproterozoic Era.

Hypothesis and Null Hypothesis

If the carbon and uranium cycles are coupled to redox, they should display a negative co-variance, with positive $\delta^{13}C$ associated with more negative $\delta^{238}U$, and vice versa. The null hypothesis states that there is no relationship between the two isotope proxies. There are several examples of this negative co-variance from middle Ediacaran successions preserving the Shuram Excursion (see Zhang et al., 2019), including the Doushantuo Formation located in South China, the Bol'shoy Patom section located in Siberia (the focus of this study), and the Johnnie Formation located in Death Valley, USA (Fig. 4). The study of the reef complex in the Chencha Formation is extremely important as the bioclasts belong to the earliest sponge-grade organisms.

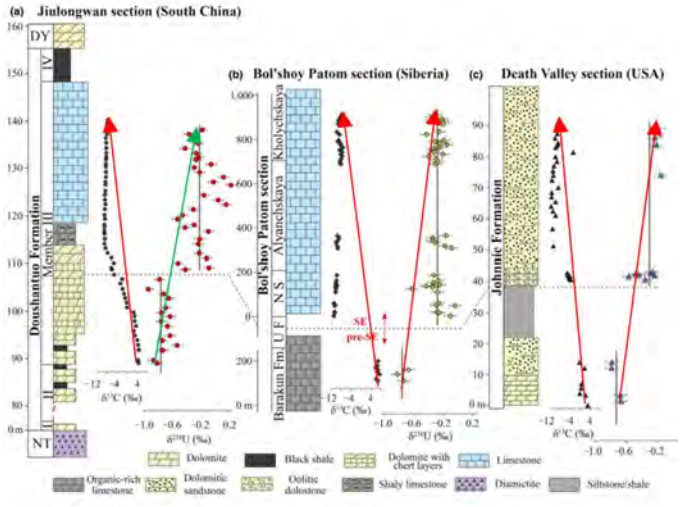

Figure 4: Stratigraphic columns from the Shuram Excursion interval in the Doushantuo Fm., Bol'shoy Patom Fm., and Johnnie Fm. that preserve strong -$\delta^{13}C$ and less negative $\delta^{238}U$ values. (modified after Zhang et al., 2019).

Therefore, determining the redox conditions preserved in this formation is imperative in the understanding of the environment in which these early animals inhabited.

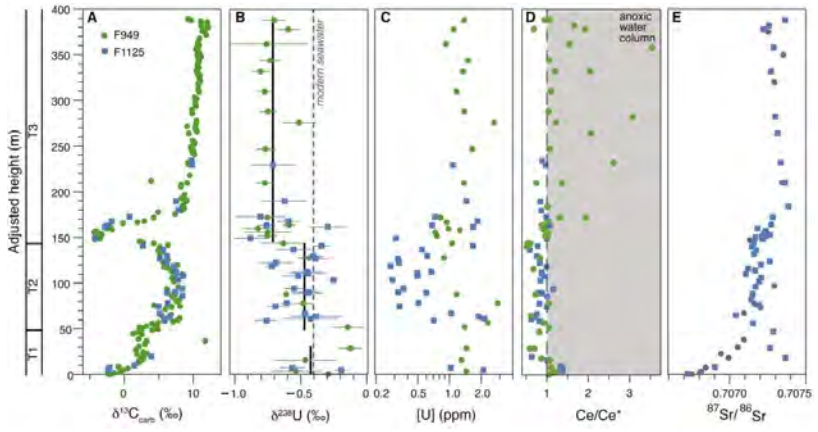

Figure 5: Plot of stratigraphic height vs. $\delta^{13}C$, $\delta^{238}U$, and U concentrations from Lau et al. (2017). The T1 section, composed of limestone, exhibits a positive shift in $\delta^{13}C$ while the mean $\delta^{238}U$ values shift to more negative values. These values continue to trend in their respective directions in the T2 section, which is composed of limestone with some oolitic, brecciated, and dolomitic interlayers. At the T2-T3 boundary a negative $\delta^{13}C$ anomaly occurs, spanning roughly 20 m, before shifting back to values of roughly 10‰. Following the negative $\delta^{13}C$ spike, the $\delta^{238}U$ values shift to even more negative values. There is a clear relationship between the positive $\delta^{13}C$ values, which increase with stratigraphic height, and the more negative $\delta^{238}U$ values, which decrease with stratigraphic height. Additionally plotted are the Ce/Ce ratios which provide the redox conditions of the overlying water column as well as Sr which reflect changes in the contributions of continental versus mantle reservoirs to ocean composition, and informs global tectonic events, weathering rates, and biogeochemical cycling.*

Conversely, carbonates that preserve positive $\delta^{13}C$ values typically preserve more negative $\delta^{238}U$ values. An example of this is preserved in the Cryogenian Taishir Formation located in Mongolia. Two stratigraphic successions exhibit the negative co-variance between increasing $\delta^{13}C$ and decreasing $\delta^{238}U$ values. Figure 5, from Lau et al., 2017, illustrates the clear relationship between the carbon and uranium isotopic values as the $\delta^{13}C$ values are strongly positive, with a negative excursion at the T2 and T3 boundary. At the same time, the $\delta^{238}U$ values are decreasing as the stratigraphic height and $\delta^{13}C$ values are increasing, with a few higher values at the T2 and T3 boundary, associated with a small negative $\delta^{13}C$ anomaly (see Lau et al., 2017). Both examples preserve anomalous $\delta^{13}C$ and $\delta^{238}U$ compositions which are similar to the values obtained in this study.

Geological Setting

Chencha Formation

Located approximately 130 km east of the city of Lensk along the Lena River, the Chencha Formation lies conformably above the Nikol'skoe Formation and unconformably below the Zherba Formation. It is a member of the Zhuya Group and the broader Patom Supergroup. This formation is characterized by its pink and white micritic, stromatolitic, and oolithic limestones in the basal layers while the upper layers are composed of silty and sandy limestones (Chumakov et al., 2011). The reef complex is roughly 8 m thick and has a very detailed lithology (Fig. 9). The basal layers are an amalgamation of limestones interbedded with mudstone, oolites, and siltstone with some cross-bedding structures indicating tidal motion. Roughly 1.5 m from the bottom of the reef complex, there appears to be the remains of some sort

Figure 6: Photo of the Chencha reef complex exposed at the top of the outcrop. Pictured is the microbial mud mounds that represent the basin margin transition from ramp to rim geometry (Alan Jay Kaufman 2021).

of water channel overlain by a layer of oolites and cross-bedded limestones and interbedded sandstones. The remaining layers are composed of oolites and alternating beds of limestone and sandstone with mudstone interbeds and bioherms. The top of the 8 m section contains bioclasts of potential sponge-grade organisms (Fig. 6). The presence of abundant oolites and crossbedding are consistent with a shallow carbonate shelf facies that is well connected to the open ocean. Pb-Pb isochron dating constrains the age of this formation to 564 ± 24 Ma (Kuznetsov pers. Comm, 2021), placing it in the terminal Ediacaran Period (Appendix A-3). More importantly, this age constraint overlaps with the Shuram Excursion, which is recorded in the Chencha and underlying Nikol'skoe formations.

Chernaya Rechka Formation

The Chernaya Rechka Formation is located approximately 13 km southeast of the city of Igarka along the Chernaya River, a tributary of the Yenisei River. Part of the greater Igarka Uplift, this formation is characterized by clayey and sandy limestones deposited in a relatively shallow to open marine facies. Throughout the formation there are varying lithotypes ranging from graded bedding to oolitic and intraclastic limestones with finely laminated shales (Fig. 11). The formation spans roughly 800 m and it unconformably overlies the Gubinskaya Formation and the Igarka volcanic complex, clasts of which are included in the conglomeritic basal layers. (Kochnev et al., 2022). The top of the formation has a gradual contact with the overlying Izluchina Formation which is composed of sandstones and siltstones. This region experienced

Figure 7: Outcrop photo of the Chernaya Rechka Formation. The outcrop shows significant amounts of deformation relating to the periods of tectonic collision and rifting throughout the Neoproterozoic. (Boris Kochnev, 2018)

periods of collision in the Meso- and Neoproterozoic as well as periods of rifting during the mid-Neoproterozoic creating narrow basins which were then infilled with volcanic and sedimentary rocks (Kochnev et al., 2022). The tectonic activity continued to pervade through the region as sections of the Chernaya Rechka Formation show significant amounts of deformation (Fig. 7). Pb-Pb isochron dating constrains the age of this formation to 610 ± 50 Ma (Appendix A-3). The uncertainty for the Chernaya Rechka is rather large placing it in either the end Cryogenian or basal Ediacaran periods.

Methods

See Appendix A-1 for a detailed methodology.

Sample collection and carbon and oxygen analysis

Samples were collected on two separate excursions to Siberia by Alan Jay Kaufman and Boris Kochnev in 2021. The Chencha Formation samples from the reef complex were transported back to UMD where they were polished and photographed. In November 2022, collaborator Natalia Bykova traveled to Toronto, Canada to deliver additional powders of stratigraphic sample through all of the Chencha and Nikol'skoe formations for isotopic analysis.

Various textures were observed on available rock chips, and these were micro-drilled to obtain ~100 μg of powder for carbon and oxygen isotopic analysis. Analyses were conducted in-house at UMD in the Paleoclimate Co-laboratory on the Multiflow Isoprime gas-source mass spectrometer (GSMS) by Laboratory Manager Jenna Wollney. The Chernaya Rechka samples were analyzed for $\delta^{13}C$ and $\delta^{18}O$ at the Geological Institute (GIN) in Moscow and organic carbon at the Siberian Scientific Research Institute of Geology, Geophysics and Mineral Raw Materials (SNIIGIMS) in Novosibirsk on a Delta V Advantage mass-spectrometer.

Uranium preparation and analysis

Following the carbon and oxygen isotopic analysis, roughly 30 g billets from both sample sets were cut and ground to remove weathered edges and saw marks, then crushed to roughly pea-sized chips in a metal-free environment. Approximately 10 g of the sample chips were powdered with an agate ball mill and placed in individual centrifuge tubes. Roughly 1.5 g of sample powder was weighed out then dissolved using a solution of trace metal grade (TMG) nitric acid (HNO_3) and left to react overnight. The following morning, solutions were centrifuged, and the supernatant was decanted into a fresh 50 mL centrifuge tube. Aliquots of each sample were taken and added gravimetrically to fresh 15 mL centrifuge tubes which were diluted up to 10 mL with 2% TMG HNO_3. Solutions were homogenized and spiked with 525 μL of 100 ppb scandium then analyzed on the Element 2 ICP-MS. Once [U] had been calculated, the amount of $^{233}U/^{236}U$ double-spike for each sample and the amount of solution to dry down was calculated. Samples were dried down and the subsequent sample digestion was initiated. The multi-day process involved several rounds of digestion in reverse aqua regia and H_2O_2. The result from the dry down step was a 3M HNO_3 solution that underwent two rounds of column chemistry at George Mason University to isolate uranium. Following the column chemistry, samples were transported to UMD where they underwent analysis on the Neptune Plus ICP-MS.

REE preparation

The REE preparation involved a sequential leaching process following (Tostevin et al., 2016). Approximately 25 mg of sample powder was weighed out and placed in fresh 15 mL centrifuge tubes. The samples were rinsed with Milli-Q water, centrifuged, and the water was discarded. Trace metal grade 2% HNO_3 was added to each sample which was then agitated and left to leach overnight. The following morning samples were centrifuged, the HNO_3 was discarded and another round of 2% HNO_3 was added to each sample. Samples were then agitated, left to leach overnight, and centrifuged the following morning. The supernatant from each sample was decanted into fresh 15 mL centrifuge tubes and diluted up to 10 mL with 2% HNO_3. Samples were then packaged and shipped off to Arizona State University where they await analysis.

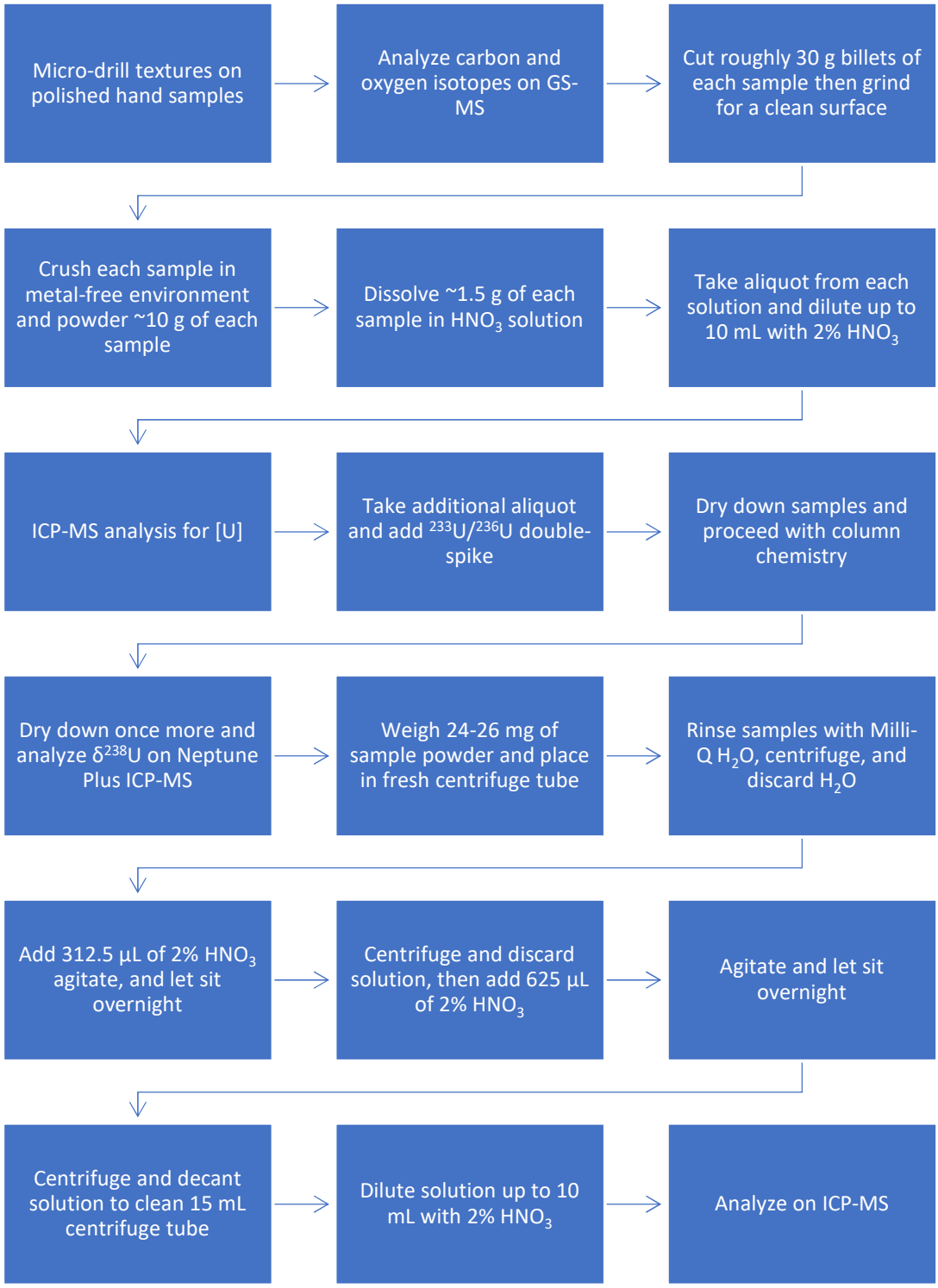

Figure 8: Simplified methods describing the various steps taken throughout the analytical process. The processes detail the carbon and oxygen isotopic analysis, followed by the uranium concentration and dissolution process, column chemistry, uranium isotopic analysis, and REE leaching procedure.

Results

	$\delta^{13}C$ (‰)	$\delta^{18}O$ (‰)	[U] (ppm)	$\delta^{238}U$ (‰)	$\delta^{13}C$ (‰)	$\delta^{13}C_{OC}$ (‰)	$\delta^{18}O$ (‰)	[U] (ppm)	$\delta^{238}U$ (‰)
Average	**-8.42**	**-9.33**	**2.64**	**-0.09**	**6.09**	**-25.03**	**-8.51**	**0.35**	**-0.55**
Uncertainties	**0.04 (JTB1) 0.06 (MCC)**	**0.09 (JTB1) 0.07 (MCC)**	**RSD: 2.4%**	**0.09**	**0.1**	**0.1**	**0.2**	**RSD: 2.4%**	**0.09**

Table 1: Averages and uncertainties for the measurements collected. The blue columns are measurements from the Chencha Formation reef complex and the orange columns are from the Chernaya Rechka Formation.

Carbon and oxygen isotope data

The results for the $\delta^{13}C$ measurements from the Chencha Formation reef complex display values that are consistent with enhanced oceanic ventilation. The formation preserves strong negative $\delta^{13}C$ values ranging between -7.8‰ and -11.1‰ with an average value of -8.4‰ (V-PDB). Average analytical uncertainties are reported as ±0.04 for the JTB1 standard and ±0.06 for the MCC standard (reported to 1σ). In addition to the $\delta^{13}C$ values, the formation also preserves strong negative $\delta^{18}O$ values ranging between -8.8‰ and -10.1‰ with an average of -9.3‰ (V-PDB) and an average analytical uncertainty of ±0.09 for the JTB1 standard and ±0.07 for the MCC standard (also reported to 1σ; see Table 1 and Fig. 9).

The Chernaya Rechka Formation exhibits strong positive $\delta^{13}C$ values ranging from -6.0‰ to 12.0‰ with an average value of 6.1‰ and a reported average analytical uncertainty of ±0.1 (2σ). There are two values at the base of the stratigraphic section that exhibit

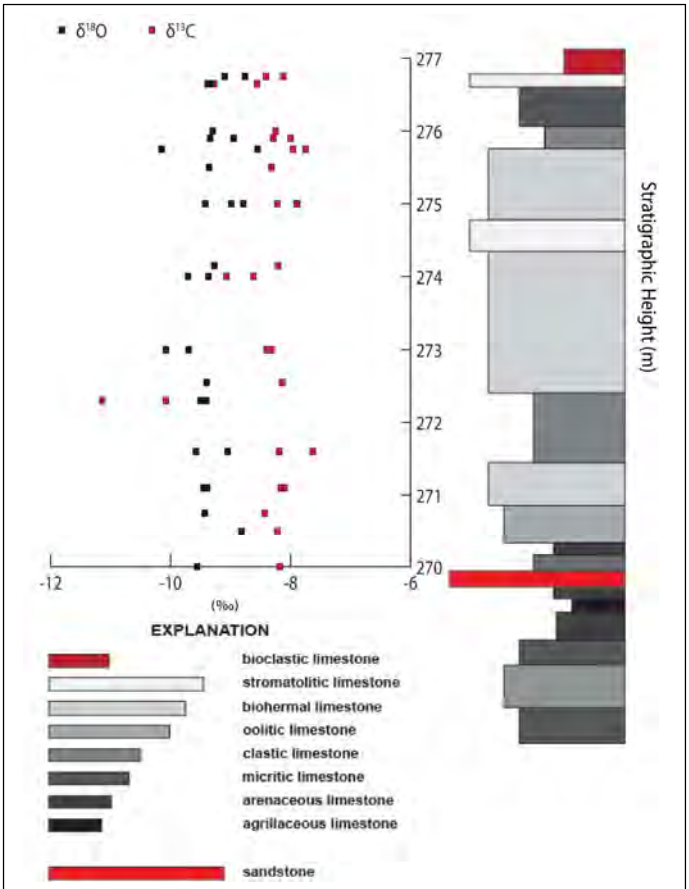

Figure 9: Chencha Formation $\delta^{13}C$ and $\delta^{18}O$ values plotted against stratigraphic height of the reef complex. $\delta^{13}C$ values range between -7.8‰ and -11.1‰. These values imply increased oceanic ventilation. The $\delta^{18}O$ values range from -8.7‰ to -10.1‰.

negative $\delta^{13}C$ values, displaying the wide shift from more oxic and ventilated conditions in the lower layers to more euxinic conditions reflected in the upper layers. The $\delta^{18}O$ values, once converted to the V-PDB standard, exhibited a range of values from -6.3‰ to -12.2‰ with an average of -8.5‰ and a reported analytical uncertainty of ±0.2 (2σ; see Table 1 for reference). The organic carbon content was measured and also serves as a diagenetic indicator. The values range between -24.9‰ and -30.3‰ with an average of -25.0‰ (Fig. 11).

Uranium concentration and $\delta^{238}U$

The [U] from the Chencha Formation reef complex exhibited a wide range of values from 0.585 to 6.80 ppm with an average [U] of 2.64 ppm and an average relative standard deviation of ±2.4% (Table 1 and Fig. 12). Conversely, values from the Chernaya Rechka Formation displayed significantly lower [U] ranging from 0.107 to 0.608 ppm with an average [U] of 0.350 ppm and an average relative standard deviation of ±2.4% (Table 1 and Fig. 12).

Uranium isotope abundances in carbonates have been used to assess the extent of euxinia in the world's oceans, which today only occupy around 0.05% of the ocean floor, specifically the Black Sea, Cariaco Basin, and Norwegian fjords (Cherry et al., 2022). Under euxinic conditions, U(IV) is preferentially removed to euxinic sediments leaving seawater U(VI) depleted in the heavy ^{238}U. In Bahamian carbonates deposited in the well-oxygenated modern ocean, the median $\delta^{238}U$ value is -0.15‰ (Chen et al., 2018). The $\delta^{238}U$ values obtained from the Chencha Reef Complex suggest an ocean that was near modern values in terms of ventilated (or oxic) conditions. The Chencha Formation preserves values as high as 0.09‰ and as low as -0.27‰ (see Fig. 13) with an average analytical uncertainty of ±0.09‰ (2σ based on replicate analyses). The Chernaya Rechka Formation preserves values as high as -0.19‰ and as low as -0.85‰ (Fig. 13), with an average $\delta^{238}U$ of -0.55‰ and an analytical uncertainty of ±0.09‰ (2σ). For lower $\delta^{238}U$ values, like those preserved in the carbonates of the Chernaya Rechka Formation, there had to have been an expansion of euxinia on a global scale. The extent to which the oceans were euxinic remains a mystery. However, even a shift of less than half a percent would create significant environmental and biological disturbances. The higher $\delta^{238}U$ values of the Chencha Formation are consistent with the higher [U] values and more negative $\delta^{13}C$ values while the more negative $\delta^{238}U$ values are consistent with the lower [U] and more positive $\delta^{13}C$ values.

Discussion

Diagenetic considerations

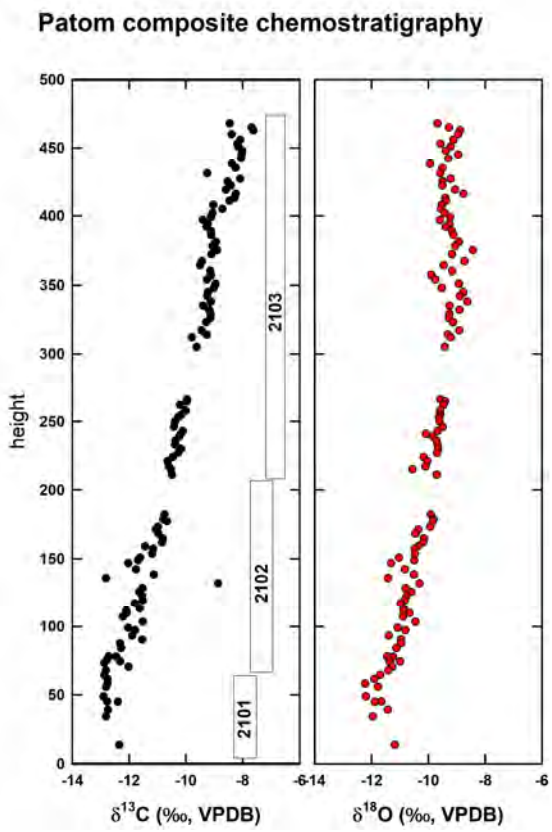

Figure 10: Chencha Formation chemostratigraphy plot from the entire formation which displays the wide range of $\delta^{13}C$ and $\delta^{18}O$ values. The $\delta^{13}C$ values in the 2101 section range from -12.9‰ to -12.3‰ with an average value of -12.7‰ and standard deviation of ±0.18‰. The $\delta^{18}O$ values in the 2101 section range from -12.2‰ to -11.7‰ with an average of -11.7‰ and a standard deviation of ±0.32‰. In the 2102 section, $\delta^{13}C$ values range from -12.9‰ to -8.8‰ with an average value of -11.6‰ and standard deviation of ±0.75‰. The $\delta^{18}O$ values in the 2102 section range from -11.4‰ to -9.8‰ with an average of -10.7‰ and a standard deviation of ±0.46‰. The $\delta^{13}C$ values in the 2103 section range from -10.6‰ to -7.6‰ with an average value of -9.2‰ and standard deviation of ±0.80‰. The $\delta^{18}O$ in the 2101 range from -10.0‰ to -8.9‰ with an average of -9.4‰ and a standard deviation of ±0.38‰ among samples. The smoothness of the curve as the stratigraphic height increases, coupled with the standard deviation (<1‰) of values in each section, suggests that the extreme negative carbon and oxygen isotopic values reflect an environmental change rather than a diagenetic change.

In the Cenozoic, $\delta^{18}O$ values of foraminifera have been used as a proxy for temperature with some assumption about seawater ^{18}O abundances, but for Neoproterozoic carbonates, oxygen isotopes have primarily been used as diagenetic indicators. For this time interval, carbonate $\delta^{18}O$ values of ca. -5‰ have been considered well preserved, while those <-10‰ are suspect (Kaufman and Knoll, 1995). The Chencha Formation reef sample $\delta^{18}O$ values are near to -10‰, which either suggests diagenetic or metamorphic alteration, warmer seawater temperature, or higher alkalinity (see Spero et al., 1997). As Knauth and Kennedy (2009) explained, carbonate rocks can isotopically re-equilibrate with higher-temperature fluids depending on the water/rock (W/R) ratios and the isotopic composition of the fluids. The W/R ratio of metamorphic fluids is typically high with respect to O and low with respect to C, so carbonate $\delta^{18}O$ is driven down through higher-temperature equilibration while $\delta^{13}C$ does not change. This implies that the low $\delta^{18}O$ values are of a diagenetic origin rather than an environmental change. However, Spero et al. (1997) suggest that $\delta^{18}O$ in carbonates is affected by high alkalinity and warmer temperatures implying that under periods with increased alkalinity and a warmer climate, $\delta^{18}O$ in carbonates will become depleted in ^{18}O, resulting in more negative values.

The $\delta^{18}O$ values observed in the Chencha Formation are consistently around -9‰. In terms of the entire reef complex and the wider stratigraphic interval, there is a coherency amongst the $\delta^{18}O$ values suggesting that the samples have not undergone significant alteration (Fig. 10). The smooth trends in both the $\delta^{13}C$ and $\delta^{18}O$ plots for the Chencha Formation likely reflect an environmental change as opposed to a diagenetic change. The Chernaya Rechka preserves $\delta^{18}O$ values that are slightly depleted and exhibit a little more variability relative to the Chencha Formation (Fig. 11). There are several factors that could influence the $\delta^{18}O$ values measured within the formation. The lithology of the Chencha Formation is predominantly limestone and relatively undeformed, while the Chernaya Rechka is limestone interbedded with shales and dolostones that have been folded (see Fig. 7). Because the Chernaya Rechka has a more diverse lithology and has undergone periods of deformation and metamorphism in certain areas, it is likely that the $\delta^{18}O$ values in the formation have been more altered than those from the Chencha. Fluids that could result in a redistribution of $\delta^{18}O$ are unlikely to redistribute $\delta^{13}C$ as they contain very little carbon and the shear amount of carbon present within the rocks themselves serves as a buffer to prevent alteration of the $\delta^{13}C$ values preserved within the rock. Further elemental analysis (such as Mn/Sr ratios) is underway and will be used as a proxy for diagenetic alteration (Kaufman and Knoll, 1995). Freshwater is rich in Mn while seawater is rich in Sr. Higher Mn/Sr ratios implies more freshwater input which corresponds to more alteration while lower Mn/Sr implies lower degrees of alteration.

As explained in Lau et al. (2017), uranium reduction in marine sediments affects both the solubility and $^{238}U/^{235}U$ of the aqueous species, changes in redox conditions should result in covarying behavior in seawater $\delta^{238}U$ and [U]. An aerial expansion of oxygenated seafloor should be reflected in more positive $\delta^{238}U$ values and higher [U] (Lau et al. 2016). The $\delta^{238}U$ values obtained in this study display a covariance with the [U] as shown by figures 10 and 11. Based on laboratory studies conducted by Chen et al. (2016) and Stirling et al. (2015), changing carbonate mineralogy can result in large differences in [U] but only small changes in the isotopic composition (Zhang et al., 2018; Lau et al., 2017). In addition, uranium can be influenced by the amount of detrital input, thus $\delta^{238}U$ is statistically correlated with [Al] as a proxy for detrital input with high detrital values corresponding to more positive $\delta^{238}U$ values (Lau et al., 2017). Yttrium and holmium ratios (Y/Ho) are also used to screen for detrital input and assess whether an authigenic seawater signal is being preserved. These analyses to assess the various proxies for diagenesis and detrital input are underway at Arizona State University.

Carbon isotopes

The canonical model for the interpretation of positive versus negative $\delta^{13}C$ values is proportional to the burial of organic matter. This interpretation is based on the assumption that negative $\delta^{13}C$ values correspond to lesser organic carbon burial, thus implying that more organic matter is being consumed and returned to the water column as DIC. Conversely, positive $\delta^{13}C$ values correspond to an enhanced flux of organic carbon burial which corresponds to greater degrees of euxinia. The $\delta^{13}C$ values of the Chencha Formation reflect a significant decrease in the flux of organic carbon burial, signifying an uptick in the remineralization of organic matter throughout the water column associated with a well-ventilated ocean. Values reach a nadir of -12‰ beneath the stratigraphic interval of this study (Fig. 4; Zhang et al., 2019) before they reach the reef complex where the values are on average -8.4‰.

The $\delta^{13}C$ values of the Chernaya Rechka Formation are on the complete opposite end of the spectrum with peak values higher than +12‰. This major swing in $\delta^{13}C$ values signifies a major shift in the organic carbon burial flux at the time this formation was deposited, implying expanded ocean euxinia. Radiometric age constraints for the Chernaya Rechka are a topic of contention as the Pb-Pb dates place it in either the end Cryogenian or early Ediacaran. The issue is that there are no known positive $\delta^{13}C$ excursions of this magnitude during the Ediacaran. However, there are major positive $\delta^{13}C$ anomalies that precede the Marinoan glaciation that are preserved in the Mongolian Taishir Formation as analyzed by Lau et al. (2017) (See Fig. 5 for reference).

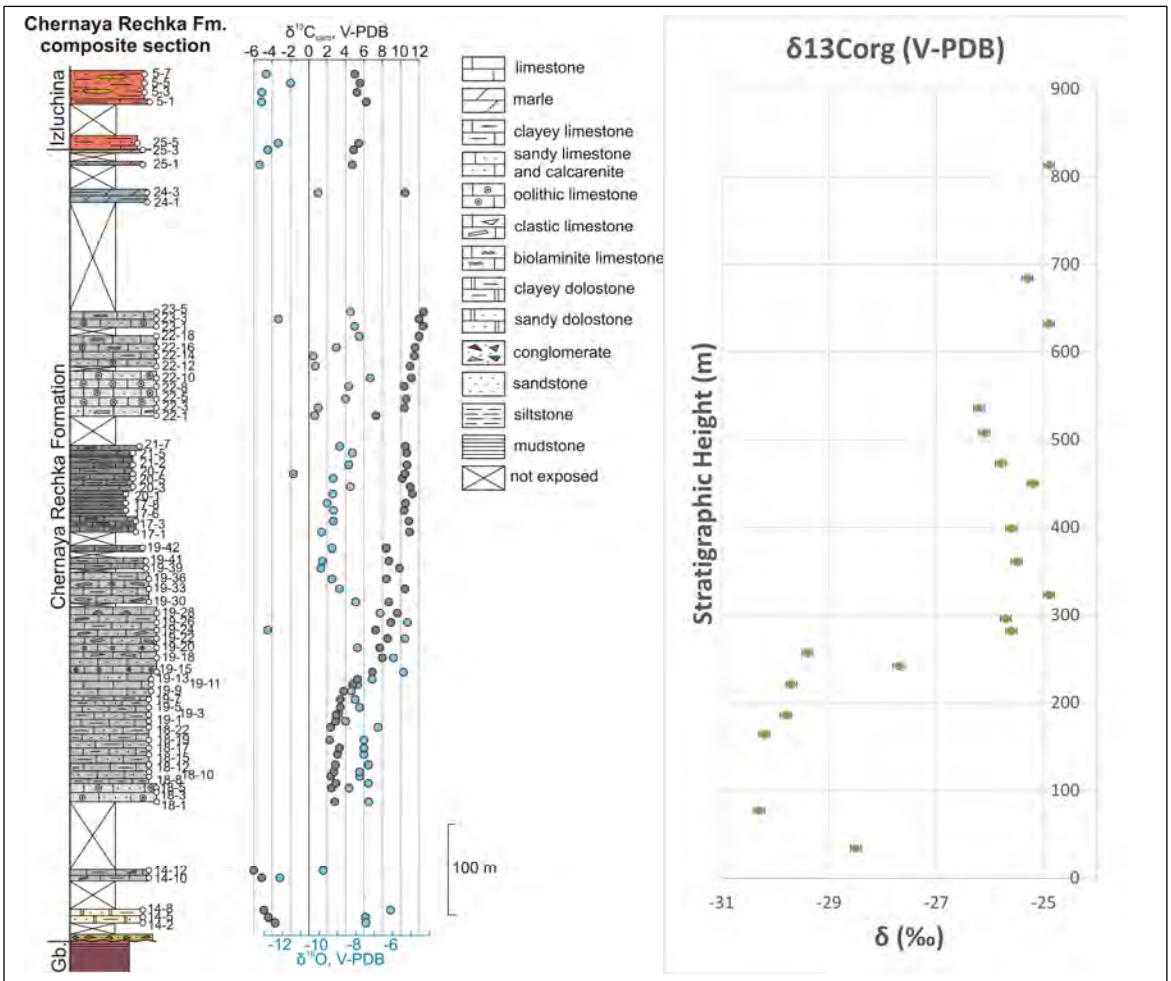

Figure 11: Chernaya Rechka chemostratigraphy plot. Shown are the $\delta^{13}C$, $\delta^{13}C_{OC}$, and $\delta^{18}O$ values. The OC and $\delta^{13}C$ show similar trends implying they were pulling from the same reservoir.

Comparing the Chencha Formation $\delta^{13}C$ values to the Chernaya Rechka Formation $\delta^{13}C$ values, it is apparent the two formations were deposited under drastically different redox conditions. The strong negative values of the Chencha Formation signify periods of enhanced oceanic ventilation likely stemming from an increase in photosynthetic processes that drive the biological pump in the world's oceans. While the oceans were more ventilated, the seawater could have been significantly buffered by the organic carbon reservoir while remaining anoxic (Rothman et al., 2003). Conversely, the strong positive values of the Chernaya Rechka

Formation imply significantly enhanced ocean euxinia, caused by the increased primary productivity through sulfate reduction, is driven by the oxidation of buried OC. This flux in organic carbon burial leaves the overlying water column enriched in ^{13}C which in turn drives a major positive shift in the $\delta^{13}C$ values.

Uranium concentrations

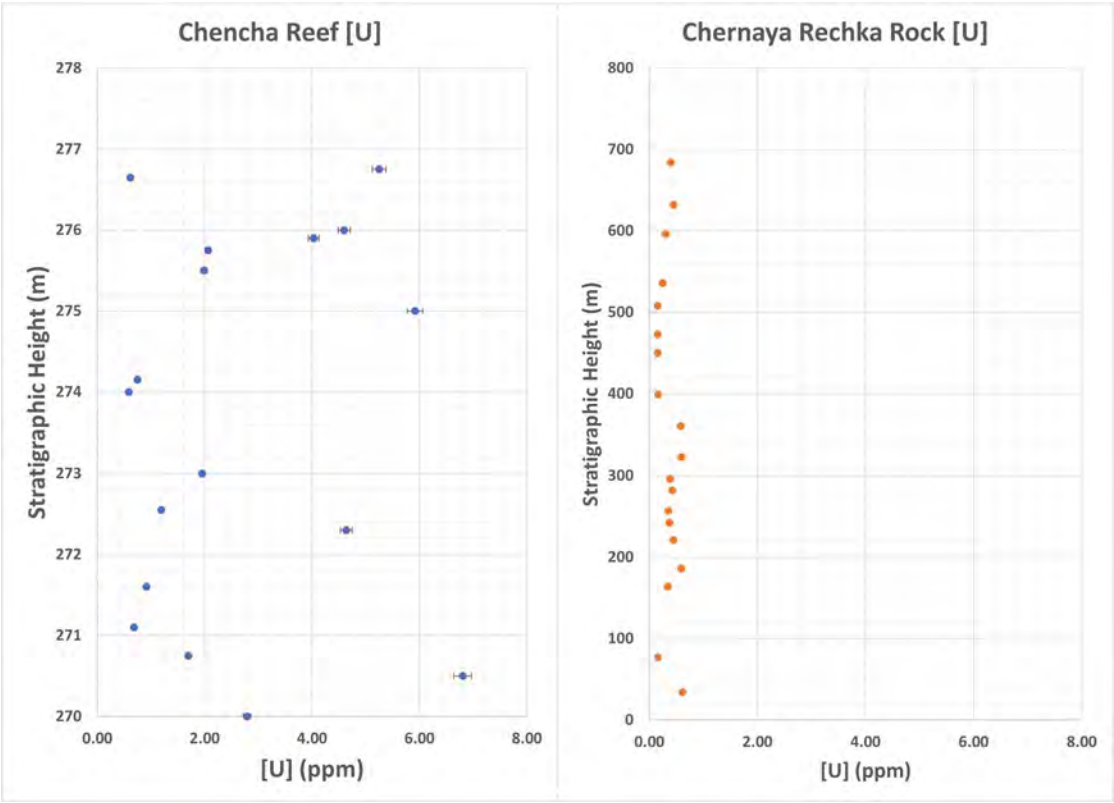

Figure 12: [U] plots that show the behavior with increasing stratigraphic height. Both samples exhibit fluctuating [U] values as the stratigraphic height increases, possibly related to shifts from aragonitic to calcitic seas.

To get a better understanding of the redox conditions in the world's oceans, uranium isotopes are used as a global indicator due to its long residence time and uniform distribution across the world's oceans. Before measuring the $\delta^{238}U$ values, the samples had to be analyzed to make sure there was a measurable amount of uranium present in the rock, and to record the concentration of uranium in each sample. The results of the [U] analysis yielded interesting results as the Chencha Formation samples exhibited an extremely high [U] with the average approximately 2.64 ppm. The average [U] for the Chernaya Rechka samples is 0.35 ppm (Table 1 and Fig. 12). These values are remarkably lower than those of the Chencha Formation and could potentially be related to the strontium content of these two formations which are remarkably high in the Chencha Formation (Pokrovskii et al., 2006) and low in the Chernaya Rechka Formation (Kochnev et al., 2022). The significant difference in [U] (and Sr) between the two formations may suggest a shift between calcite and aragonite seas. Based on Chen et al. (2016), previous experiments conducted on uranium isotope fractionation during the

coprecipitation with aragonite and calcite, aragonite exhibits significantly higher [U] when compared to calcite. The drastically different concentrations appear to possibly be linked to crystal structure and the ability for the large uranium cations to undergo a coupled substitution in the mineral structures. The reason aragonite may exhibit higher [U] than calcite may be attributed to its orthorhombic structure which is significantly more accommodating for those larger uranium cations than calcite's trigonal structure.

Uranium Isotopes

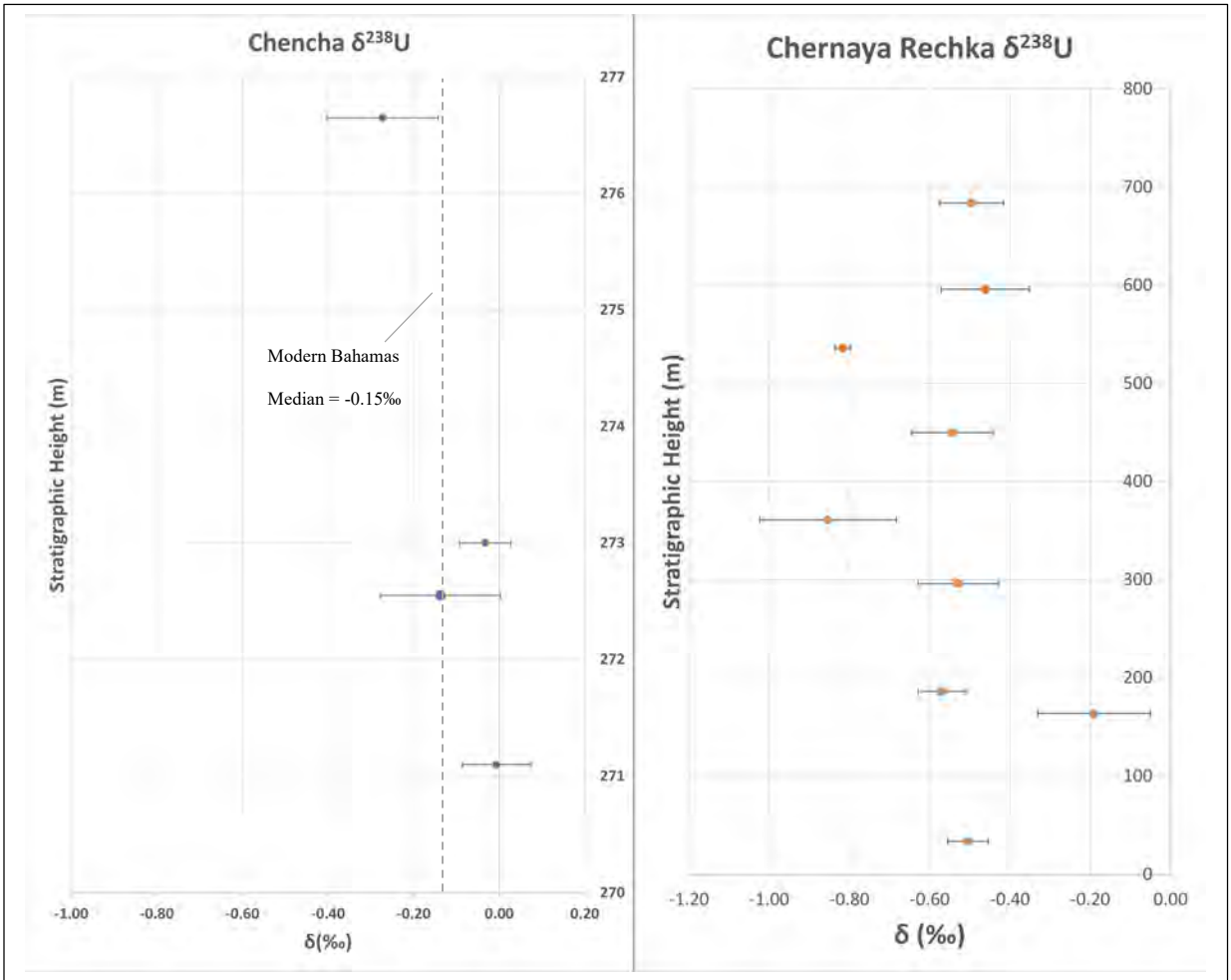

Figure 13: $\delta^{238}U$ plots for the Chencha Formation reef complex (left) and the Chernaya Rechka Formation (right). The Chencha Formation $\delta^{238}U$ values are consistent with present-day carbonate $\delta^{238}U$ values implying they were deposited under well-ventilated (and oxic) conditions. The Chernaya Rechka Formation $\delta^{238}U$ values are significantly more negative implying the oceans were significantly more euxinic than the present day.

In the Chencha Formation, the $\delta^{238}U$ values are on average -0.09‰, which is near modern carbonate $\delta^{238}U$ values while the [U] is, on average, 2.64 ppm. Conversely, the Chernaya Rechka Formation displays more negative $\delta^{238}U$ values, on average -0.55‰, while the [U] in the studied sections of the formation is, on average, 0.35 ppm. The general trend between the $\delta^{238}U$ values and [U] in the two formations is that as one increases, the other also increases, and vice versa.

The $\delta^{238}U$ values measured in the Chencha Formation are consistent with a well-ventilated (and oxic) ocean, suggesting that the Shuram Excursion represents a major shift from widespread euxinia to a significantly more ventilated (and oxic) ocean (Fig. 13). Compared to Zhang et al. (2018), the $\delta^{238}U$ values obtained in this study were slightly heavier implying the reef complex, which has not been previously recognized in literature, has something driving these heavier values. The 2021 discovery of sponge-grade bioclasts within the reef complex may be the key to understanding the redox conditions of the world's oceans at this time. If the sponges suddenly appeared in the reef, they would affect the water column by filtering the organic matter which would clear the water column, thus strengthening photosynthetic processes. This would then lead to greater buildup of oxygen in the water column, which would subsequently drive the $\delta^{238}U$ to heavier values. However, as suggested by Cherry et al. (2022), the oxygenation of the Ediacaran oceans was not a "one-off" event, rather, the post-Shuram oceans oscillated back and forth between expanded euxinia and expanded ventilation throughout the remainder of the Ediacaran Period. So, while the oceans may have experienced a period of oxygenation, this would only be a temporary event before they shifted back to more euxinic conditions based on U isotope studies worldwide.

Conversely, the $\delta^{238}U$ values in the Chernaya Rechka Formation are much more negative implying a global expansion of euxinia throughout the world's oceans. Because euxinic

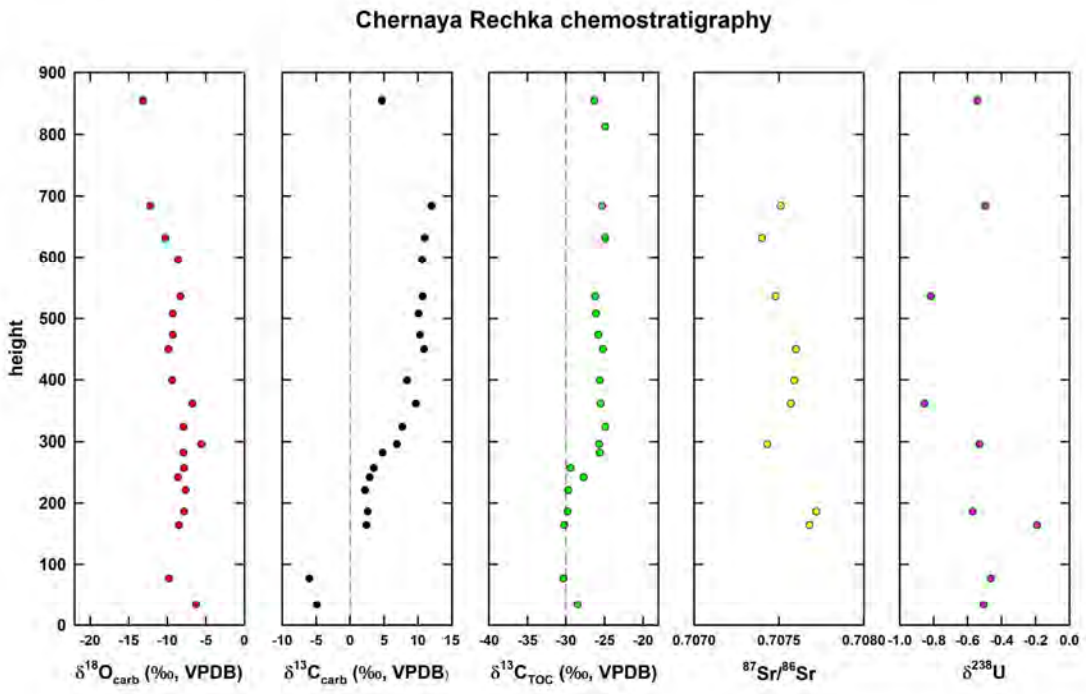

Figure 14: Chemostratigraphic profile of the Chernaya Rechka Formation. Carbon, oxygen, strontium and uranium values provide an insight into the global redox conditions at the time this formation was deposited. The values observed are consistent with those in Fig. 5 from Lau et al. (2017). The fit of these values to those from the Taishir Formation suggest that the Chernaya Rechka is a Cryogenian formation rather than an early Ediacaran succession.

sediments, which preferentially sequester the isotopically heavy ^{238}U, are the largest sink for seawater uranium, a negative shift in the $\delta^{238}U_{carb}$ suggests the expansion of global euxinia in the oceans (Fig. 13). A small change in the size of the euxinic pool in the ocean is enough to have a drastic effect on biological life. The $\delta^{238}U$ values and positive $\delta^{13}C$ values analyzed in the Chernaya Rechka Formation appear to be consistent with those analyzed by Lau et al. (2017), in the Cryogenian Taishir Formation of Mongolia. As mentioned in the carbon isotope discussion section, the age constraints for the Chernaya Rechka Formation are contested as the wide uncertainty associated with the Pb-Pb radiometric dates places the formation at either the terminal Cryogenian or basal Ediacaran Period. The issue with the emplacement of the formation in the lower Ediacaran is the lack of extended periods of such positive $\delta^{13}C$ anomalies and generally more radiogenic $^{87}Sr/^{86}Sr$ than in the Cryogenian. The $\delta^{238}U$, $\delta^{13}C$, and $^{87}Sr/^{86}Sr$ values analyzed in the Chernaya Rechka Formation appear to be consistent with those analyzed by Lau et al. (2017) in the Taishir Formation (see Figures 5 and 14 for reference). Based off a comparative analysis of the strata in Mongolia and Siberia, the Chernaya Rechka Formation appears to better fit in with the late Cryogenian, as opposed to the early Ediacaran.

The $\delta^{13}C$ and $\delta^{238}U$ values obtained in both the Chencha Formation and Chernaya Rechka Formation display a clear inverse relationship that demonstrate the two endmembers of the ever-shifting redox in the Precambrian oceans. The working hypothesis that more positive $\delta^{13}C$ values would correspond to more negative $\delta^{238}U$ values and more negative $\delta^{13}C$ values correspond to heavier (less negative) $\delta^{238}U$ values has been verified.

Conclusions

The relationship between the near modern $\delta^{238}U$ values and the negative $\delta^{13}C$ values of the Chencha Formation suggests a causal link between the perturbation to the carbon cycle caused by the Shuram Excursion and shifting redox conditions. The $\delta^{18}O$ values obtained rule out a diagenetic explanation (Appendix A-7: Fig. 20-22) and thus imply the excursion may be related to the increased circulation of the lighter and significantly more abundant ^{12}C throughout the oceans as alkalinity formed through the anaerobic oxidation of organic matter. The shifting redox conditions, coupled with the discovery of sponge-grade bioclasts within the Chencha Formation suggest the potential for biological controls on the ventilation of the oceans. On the other hand, the significantly more negative $\delta^{238}U$ values and positive $\delta^{13}C$ values associated with the Chernaya Rechka Formation may be attributed to increased primary productivity and burial of organic matter, leaving the overlying water column enriched in the heavier ^{13}C isotope, and driving the carbonate $\delta^{13}C$ to considerably more positive values. The analysis of REE in both formations will provide insight into the local redox of the overlying water column and play a key role in screening for diagenesis.

Based on the results of the carbon and oxygen isotope analyses, samples from the two formations exhibit drastically different values with the Chencha Formation exhibiting a significantly negative $\delta^{13}C$ trend while the Chernaya Rechka samples exhibit a strongly positive $\delta^{13}C$ trend. The two opposite values may be relating to increased primary productivity, which would increase the flux of organic carbon burial, thus creating a reservoir that is enriched in the heavier ^{13}C, driving more positive $\delta^{13}C$ values. Conversely, the more negative $\delta^{13}C$ is associated with increased oceanic ventilation and oxygenation implying that the biological pump was circulating more ^{12}C throughout the reservoir driving the $\delta^{13}C$ to more negative values. The [U]

values of the Chencha Formation are significantly higher than the Chernaya Rechka which may be related to calcite versus aragonite seas under which these two successions were deposited. The orthorhombic crystal structure of aragonite is able to accommodate a coupled substitution for the large uranium cation while the trigonal structure of calcite is not as accommodating for those larger cations.

The $\delta^{238}U$ values preserved in the carbonates provide a global redox profile of the world's oceans during these two critical intervals of Earth history. The negative $\delta^{13}C$ values and less negative $\delta^{238}U$ values in the Chencha Formation, and the positive $\delta^{13}C$ and more negative $\delta^{238}U$ values from the Chernaya Rechka Formation, verify the hypothesis that more negative $\delta^{13}C$ preserved in marine carbonates would be characterized by less negative $\delta^{238}U$ values and vice versa. Having discussed the diagenetic considerations and significance of the findings, I have confidence that the isotope concentrations are directly related to the depositional compositions. The results from the carbon and uranium isotopic analyses are consistent with previous studies but adds new dimensions to our understandings of the deep-time carbon and uranium cycles.

References

Blank, J. G., Delaney, J. R., & Marais, D. J. D. (1993). The concentration and isotopic composition of carbon in basaltic glasses from the Juan de Fuca Ridge, Pacific Ocean. *Geochimica Et Cosmochimica Acta*, *57*(4), 875–887. https://doi.org/10.1016/0016-7037(93)90175-v

Broecker, W. S. (1970). A boundary condition on the evolution of atmospheric oxygen. *Journal of Geophysical Research*, *75*(18), 3553–3557. https://doi.org/10.1029/jc075i018p03553

Canfield, D. E., Poulton, S. W., & Narbonne, G. M. (2007). Late-Neoproterozoic deep-ocean oxygenation and the rise of Animal Life. *Science*, *315*(5808), 92–95. https://doi.org/10.1126/science.1135013

Chen, X., Romaniello, S. J., Herrmann, A. D., Hardisty, D., Gill, B. C., & Anbar, A. D. (2018). Diagenetic effects on uranium isotope fractionation in carbonate sediments from the Bahamas. *Geochimica Et Cosmochimica Acta*, *237*, 294–311. https://doi.org/10.1016/j.gca.2018.06.026

Chen, X., Romaniello, S. J., Herrmann, A. D., Wasylenki, L. E., & Anbar, A. D. (2016). Uranium isotope fractionation during coprecipitation with aragonite and calcite. *Geochimica Et Cosmochimica Acta*, *188*, 189–207. https://doi.org/10.1016/j.gca.2016.05.022

Cherry, L. B., Gilleaudeau, G. J., Grazhdankin, D. V., Romaniello, S. J., Martin, A. J., & Kaufman, A. J. (2022). A diverse Ediacara assemblage survived under low-oxygen conditions. *Nature Communications*, *13*(1). https://doi.org/10.1038/s41467-022-35012-y

Chumakov, N. M., Pokrovsky, B. G., & Melezhik, V. A. (2011). Chapter 27 the glaciogenic Bol'shoy Patom Formation, Lena River, Central Siberia. *Geological Society, London, Memoirs*, *36*(1), 309–316. https://doi.org/10.1144/m36.27

Condon, D., Zhu, M., Bowring, S., Wang, W., Yang, A., & Jin, Y. (2005). U-Pb ages from the Neoproterozoic Doushantuo Formation, China. *Science*, *308*(5718), 95–98. https://doi.org/10.1126/science.1107765

De Baar, H. J. W. (1991). On cerium anomalies in the Sargasso Sea. *Geochimica Et Cosmochimica Acta*, *55*(10), 2981–2983. https://doi.org/10.1016/0016-7037(91)90463-f

De Baar, H. J. W., Bacon, M. P., Brewer, P. G., & Bruland, K. W. (1985). Rare earth elements in the Pacific and Atlantic Oceans. *Geochimica Et Cosmochimica Acta*, *49*(9), 1943–1959. https://doi.org/10.1016/0016-7037(85)90089-4

De Carlo, E. H., & Green, W. J. (2002). Rare earth elements in the water column of Lake Vanda, McMurdo Dry Valleys, Antarctica. *Geochimica Et Cosmochimica Acta*, *66*(8), 1323–1333. https://doi.org/10.1016/s0016-7037(01)00861-4

Derry, L. A. (2010). A burial diagenesis origin for the Ediacaran Shuram–Wonoka carbon isotope anomaly. *Earth and Planetary Science Letters*, *294*(1-2), 152–162. https://doi.org/10.1016/j.epsl.2010.03.022

Evans, M. N., Selmer, K. J., Breeden, B. T., Lopatka, A. S., & Plummer, R. E. (2016). Correction algorithm for online continuous flow $\delta^{13}C$ and $\delta^{18}O$ carbonate and cellulose stable isotope analyses. *Geochemistry, Geophysics, Geosystems*, *17*(9), 3580–3588. https://doi.org/10.1002/2016gc006469

Grazhdankin, D. V., Balthasar, U., Nagovitsin, K. E., & Kochnev, B. B. (2008). Carbonate-hosted Avalon-type fossils in Arctic Siberia. *Geology*, *36*(10), 803. https://doi.org/10.1130/g24946a.1

Grotzinger, J. P., Fike, D. A., & Fischer, W. W. (2011). Enigmatic origin of the largest-known carbon isotope excursion in Earth's history. *Nature Geoscience*, *4*(5), 285–292. https://doi.org/10.1038/ngeo1138

Hayes, J. M., (1983) Geochemical evidence bearing on the origin of aerobiosis, a speculative hypothesis.

Kaufman, A. J., & Knoll, A. H. (1995). Neoproterozoic variations in the C-isotopic composition of seawater: Stratigraphic and biogeochemical implications. *Precambrian Research*, *73*(1-4), 27–49. https://doi.org/10.1016/0301-9268(94)00070-8

Knauth, L. P., & Kennedy, M. J. (2009). The late Precambrian greening of the Earth. *Nature*, *460*(7256), 728–732. https://doi.org/10.1038/nature08213

Kochnev, B. B., Khudoley, A. K., Priyatkina, N. S., Andrew Dufrane, S., Pokrovsky, B. G., Kuznetsov, A. B., Kaurova, O. K., & Marusin, V. V. (2022). Neoproterozoic evolution of the northwestern margin of the Siberian platform. *Precambrian Research*, *382*, 106877. https://doi.org/10.1016/j.precamres.2022.106877

Lau, K. V., Macdonald, F. A., Maher, K., & Payne, J. L. (2017). Uranium isotope evidence for temporary ocean oxygenation in the aftermath of the Sturtian Snowball Earth. *Earth and Planetary Science Letters*, *458*, 282–292. https://doi.org/10.1016/j.epsl.2016.10.043

Lau, K. V., Maher, K., Altiner, D., Kelley, B. M., Kump, L. R., Lehrmann, D. J., Silva-Tamayo, J. C., Weaver, K. L., Yu, M., & Payne, J. L. (2016). Marine anoxia and delayed Earth system recovery after the end-Permian extinction. *Proceedings of the National Academy of Sciences*, *113*(9), 2360–2365. https://doi.org/10.1073/pnas.1515080113

Nelson, L. L., Ahm, A.-S. C., Macdonald, F. A., Higgins, J. A., & Smith, E. F. (2021). Fingerprinting local controls on the Neoproterozoic carbon cycle with the isotopic record of Cryogenian carbonates in the Panamint Range, California. *Earth and Planetary Science Letters*, *566*, 116956. https://doi.org/10.1016/j.epsl.2021.116956

Pokrovskii, B. G., Melezhik, V. A., & Bujakaite, M. I. (2006). Carbon, oxygen, strontium, and sulfur isotopic compositions in late Precambrian rocks of the Patom Complex, central Siberia: Communication 1. results, isotope stratigraphy, and dating problems. *Lithology and Mineral Resources*, *41*(5), 450–474. https://doi.org/10.1134/s0024490206050063

Pu, J. P., Bowring, S. A., Ramezani, J., Myrow, P., Raub, T. D., Landing, E., Mills, A., Hodgin, E., & Macdonald, F. A. (2016). Dodging snowballs: Geochronology of the Gaskiers glaciation and the first appearance of the Ediacaran Biota. *Geology*, *44*(11), 955–958. https://doi.org/10.1130/g38284.1

Rooney, A. D., Cantine, M. D., Bergmann, K. D., Gómez-Pérez, I., Al Baloushi, B., Boag, T. H., Busch, J. F., Sperling, E. A., & Strauss, J. V. (2020). Calibrating the coevolution of Ediacaran life and environment. *Proceedings of the National Academy of Sciences*, *117*(29), 16824–16830. https://doi.org/10.1073/pnas.2002918117

Rothman, D. H., Hayes, J. M., & Summons, R. E. (2003). Dynamics of the Neoproterozoic carbon cycle. *Proceedings of the National Academy of Sciences*, *100*(14), 8124–8129. https://doi.org/10.1073/pnas.0832439100

Sahoo, S. K., Planavsky, N. J., Jiang, G., Kendall, B., Owens, J. D., Wang, X., Shi, X., Anbar, A. D., & Lyons, T. W. (2016). Oceanic oxygenation events in the anoxic Ediacaran Ocean. *Geobiology*, *14*(5), 457–468. https://doi.org/10.1111/gbi.12182

Saltzman, M. R., & Thomas, E. (2012). Carbon isotope stratigraphy. *The Geologic Time Scale*, 207–232. https://doi.org/10.1016/b978-0-444-59425-9.00011-1

Shields, G. A., Mills, B. J., Zhu, M., Raub, T. D., Daines, S. J., & Lenton, T. M. (2019). Unique Neoproterozoic carbon isotope excursions sustained by coupled evaporite dissolution and pyrite burial. *Nature Geoscience*, *12*(10), 823–827. https://doi.org/10.1038/s41561-019-0434-3

Spero, H. J., Bijma, J., Lea, D. W., & Bemis, B. E. (1997). Effect of seawater carbonate concentration on foraminiferal carbon and oxygen isotopes. *Nature*, *390*(6659), 497–500. https://doi.org/10.1038/37333

Stirling, C. H., Andersen, M. B., Warthmann, R., & Halliday, A. N. (2015). Isotope fractionation of 238U and 235U during biologically-mediated uranium reduction. *Geochimica Et Cosmochimica Acta*, *163*, 200–218. https://doi.org/10.1016/j.gca.2015.03.017

Tissot, F. L. H., & Dauphas, N. (2015). Uranium isotopic compositions of the crust and ocean: Age corrections, U budget and global extent of modern anoxia. *Geochimica Et Cosmochimica Acta*, *167*, 113–143. https://doi.org/10.1016/j.gca.2015.06.034

Tostevin, R., Shields, G. A., Tarbuck, G. M., He, T., Clarkson, M. O., & Wood, R. A. (2016). Effective use of cerium anomalies as a redox proxy in carbonate-dominated marine settings. *Chemical Geology*, *438*, 146–162. https://doi.org/10.1016/j.chemgeo.2016.06.027

Zhang, F., Xiao, S., Kendall, B., Romaniello, S. J., Cui, H., Meyer, M., Gilleaudeau, G. J., Kaufman, A. J., & Anbar, A. D. (2018). Extensive marine anoxia during the terminal Ediacaran Period. *Science Advances*, *4*(6). https://doi.org/10.1126/sciadv.aan8983

Zhang, F., Xiao, S., Romaniello, S. J., Hardisty, D., Li, C., Melezhik, V., Pokrovsky, B., Cheng, M., Shi, W., Lenton, T. M., & Anbar, A. D. (2019). Global marine redox changes drove the rise and fall of the Ediacara biota. *Geobiology*, *17*(6), 594–610. https://doi.org/10.1111/gbi.12359

Acknowledgements

I would like to thank Dr. Alan Jay Kaufman for advising me for the past year and providing guidance to ensure that the project ran smoothly, Dr. Philip Piccoli for providing guidance in the navigation of the Senior Thesis process, Geoffrey J Gilleaudeau for analytical, and facilities support, Tian Gan for analytical support, Our Russian colleagues for research support, Jenna Wollney for analytical support, Dr. Richard Ash for analytical support and facilities, Igor Puchtel for facilities support, and Tyler from Arizona State University for analytical and facilities support.

Competing interests statement

I, Matthew G. Pedersen, declare no competing interests.

Honor Code

I pledge on my honor that I have not given or received any unauthorized assistance or plagiarized on this assignment.

Appendix

A-1:

Methods

Sample Preparation for Carbon and Oxygen Analysis

Samples were collected on two separate excursions to Russia. The Chencha Formation samples were gathered by Dr. Alan Jay Kaufman in 2021 and the Chernaya Rechka samples were collected by Boris Kochnev in 2018. Hand samples were cut with an MK saw and polished on one side using a Labopol grinding wheel starting with 80 grit sandpaper and finishing with 550 grit and then photographed with a scale. The textures of the Chencha Formation samples were observed and micro-drilled for carbon and oxygen isotope analysis. The samples were

analyzed in the University of Maryland Paleoclimate Co-Laboratory with a Multiflow inlet system in-line with a Isoprime gas source mass spectrometer by Laboratory Manager Jenna Wollney (Fig. 15).

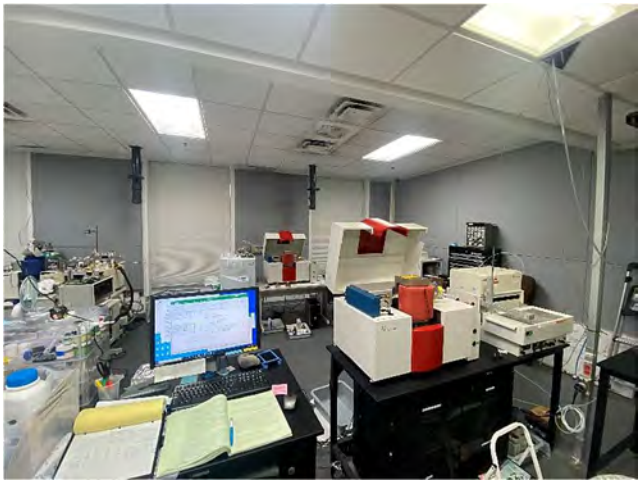

Figure 15: Image from inside the Paleoclimate Co-Laboratory. Shown is the Isoprime gas source mass spectrometer where the $\delta^{13}C$ $\delta^{18}O$ data was gathered for the Chencha Formation samples.

Two standards were used in conjunction with the analysis, JTB1, which has a higher range of $\delta^{13}C$ and $\delta^{18}O$ values, and MCC, which has a much lower range of $\delta^{13}C$ and $\delta^{18}O$ values. Raw data underwent a series of corrections with the first being a spline correction to account for drift in the raw values across the run. Next, an amplitude correction was applied to the data to account for varying amounts of carbonate in each sample. Lastly, a two-point correction was applied to partially corrected data which converted the values to known (calibrated against IAEA-CO-1, LSVEC, JTB-1, and MCC) values using the following equation:

$$X_{known} = a + b * X_{measured}$$

where a and b are coefficients calculated from the two-point regression of known values of JTB-1 and MCC relative to international standards IAEA-CO-1 and LSVEC on the V-PDB scale versus working standard values measured in the specific batch of analyses (Evans et al., 2016). Once a and b were estimated, the measured values were converted to the V-PDB scale (see Evans et al., 2016). On the day of analysis for the Chencha Formation samples, the associated uncertainties were ±0.04 for $\delta^{13}C$ and ±0.09 for $\delta^{18}O$ for the JTB1 standard. The uncertainties were ±0.06 for $\delta^{13}C$ and ±0.07 for $\delta^{18}O$ using the MCC standard. All values of the known standards are of 1σ precision and fall within an acceptable standard deviation.

The Chernaya Rechka Formation samples were measured in Russia with the $\delta^{13}C$ and $\delta^{18}O$ measurements done at the Geological Institute (GIN) in Moscow on the Thermoelectron Delta V Advantage with Gas Bench II. Reported uncertainties for the $\delta^{18}O$ and $\delta^{13}C$ are ±0.2 and ±0.1 respectively. $\delta^{18}O$ values were measured using the V-SMOW standard which had to be converted to V-PDB standards through the following equation:

$$\delta^{18}O_{V-PD} = \frac{\delta^{18}O_{V-SMOW} - 30.86}{1.03086}$$

Organic carbon (OC) was measured at the Siberian Scientific Research Institute of Geology, Geophysics and Mineral Raw Materials (SNIIGIMS) in Novosibirsk on the Delta V Advantage mass-spectrometer.

Supernatant preparation

Surfaces of roughly 30 g billets from both sample sets were ground with the Labopol grinding wheels to remove weathered surfaces and metal saw marks and were then crushed in a metal-free environment to roughly pea-sized pebbles. These were placed in an agate ball mill for a 10-minute cycle where they were reduced to a fine powder. Powders were stored in 6M hydrochloric acid (HCl) leached, 50 mL centrifuge tubes. The empty tube + cap weight was recorded and approximately 1.5 g of powder from each sample was added to individual centrifuge tubes. These were then slowly and sequentially acidified with 20 mL of 1M trace metal grade (TMG) nitric acid (HNO_3), 5 mL of concentrated (16M) TMG HNO_3, and 15 mL of 1M TMG HNO_3. The solutions were then vortexed and allowed to react overnight. The next morning samples were centrifuged at 5000 rpm for 10 minutes and the supernatant decanted into fresh acid-leached 50 mL centrifuge tubes. The residues were rinsed with 18.2 MΩ Milli-Q water several times and then placed in a drying oven at 60°C to dry overnight. Once dry, the weight of the tube + cap + residue was recorded, and the percentage of carbonate calculated.

Uranium concentration preparation

For the uranium isotope concentration measurements, ~9.8 mL of 2% HNO_3 was added gravimetrically to a 15 mL centrifuge tube followed by a ~200 µL aliquot from each sample solution. The solution was spiked with 525 µL of 100 ppb scandium, homogenized, and then ~2 mL was poured into sample wells for uranium abundance analysis along with concentration standards of U, Sc, and Ca, on the Element 2 Inductively Coupled Plasma Mass Spectrometer (ICP-MS; Appendix A-4) with the assistance of Dr. Richard Ash.

To calculate [U], the following had to occur:

1.) Once the three standards (calcium, scandium, and uranium) were run, a linear trendline was generated with the standard concentrations in parts per billion along the y-axis and the number of counts per second (cps) on the x-axis.
2.) The equation of the slope of the line was calculated, the cps data for uranium was input into the equation which yielded the uncorrected U concentration values (Fig. 16).
3.) To account for decreases in sensitivity, a correction algorithm had to be applied to the samples (Appendix A-5).
4.) The last step was calculating the amount of U in the total rock using the following equation:

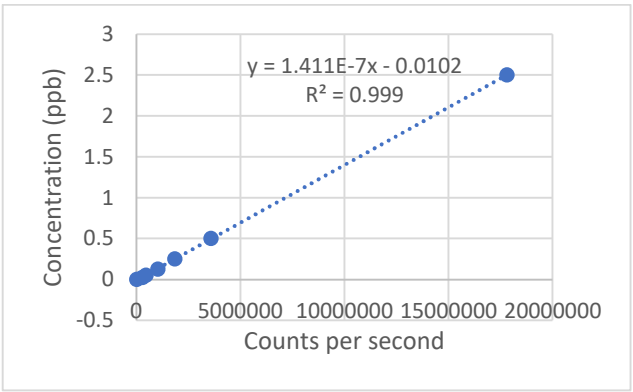

Figure 16: Calibration curve for U concentrations on the Element 2 ICP-MS analyzer. If the machine is properly calibrated, the line will increase linearly as opposed to exponentially. The line is scaled up or down depending on the concentrations of material being analyzed.

$$Rock\ U\ (ppm) = \left(\frac{\frac{final\ mL\ weight}{aliquot\ mL\ weight} * \frac{mL\ dissolved}{powder\ weight}}{1000} \right) * U_{concentration}$$

The [U] was used to determine the exact double spike ($^{233}U/^{236}U$: 0.8 mL for every 500 ng of U) amount to be added to the solutions.

Preparation for uranium isotope analysis

Additional aliquots were taken and added gravimetrically using the prior method and the amount of solution in mL to dry down was calculated from the U concentrations. Samples were dried down on a hot plate at 180ºC then spiked with the calculated amount of the $^{233}U/^{236}U$ double-spike. After the double-spike was added, samples were placed back on the hot plate at 180ºC and dried down overnight and removed in the morning. A 6 mL solution of reverse aqua regia (4.5 mL concentrated trace metal grade HNO3 and 1.5 mL HCl) was added to the samples which were then capped and put back on the hot plate at 180ºC overnight. In the morning they were uncapped and partially dried down so that less than 1 mL of solution was in the Teflon beaker. Samples that had undissolved solids in the solution underwent another round of reverse aqua regia. Once no undissolved particles remained in the solution, 2 mL of concentrated TMG HNO_3 and 0.2 mL of 30% hydrogen peroxide (H_2O_2) was added to the samples which were then capped and left on a hot plate over night at 180ºC. In the morning they were removed and let cool then placed back on the hot plate, un-capped, where they were partially dried down again. This process was repeated until no undigested particles remained and everything was in solution.

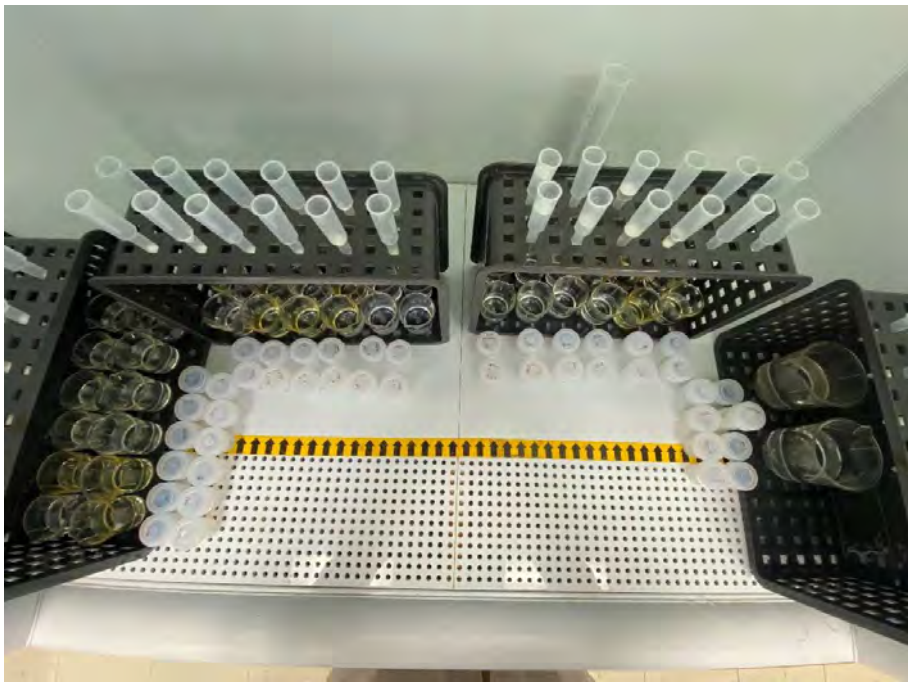

Figure 17: Ion exchange chromatography setup at GMU. In addition to the Chencha and Chernaya Rechka formations, additional samples from the Bitter Springs Formation (part of a separate project) also underwent ion exchange chromatography. This step shows the samples in the columns being separated in the first round using the UTEVA resin.

After the partial dry down, 2 mL of concentrated TMG HNO_3 was added to the samples which were capped and placed on the hot plate overnight. In the morning samples were removed, cooled, and placed on the hot plate for

one final partial dry down. After this step, each sample received 10 mL of 3M TMG HNO_3 and was then capped and placed on the hot plate overnight. In the morning samples were removed and let cool then transported to George Mason University (GMU) for ion exchange chromatography (Fig. 17).

When preparing the samples in this step for uranium isotope analysis, UTEVA (Uranium and TetraValents Actinides) resin is used. The purpose of the UTEVA resin is to run a liquid solution through the resin and only specific elements will bind to that resin. In this scenario, only uranium and thorium bind to the resin with the latter being removed by running a solution of 5M HCl and 0.05M oxalic acid through the column. A second column was run using DGA resin which removes any excess calcium and sodium to minimize any decreases in sensitivity in the Neptune Plus during analysis. What is left after the two column procedures is roughly 10 mL of a 0.05M HCl solution containing pure uranium.

Neptune Plus ICP-MS analysis

Upon the conclusion of the ion exchange chromatography, samples were returned to UMD, where they underwent several analytical sessions on the Neptune Plus ICP-MS to measure the $\delta^{238}U$ of several samples from each set (Fig. 18).

To calculate $\delta^{238}U$, the following equation was used:

$$\delta^{238}U = [(({}^{238}U/{}^{235}U)_{sample}/({}^{238}U/{}^{235}U)_{standard}) - 1] \times 10^3$$

Figure 18: Neptune Plus ICP-MS at the University of Maryland, College Park.

where the ratio of ^{238}U to ^{235}U in the sample was divided by the ratio of ^{238}U to ^{235}U in a standard. Standards are used for all isotopic analyses as values from each mass spectrometer vary depending on the instrument. In this analytical session, there were two standards used, Certified Reference Material (CRM)-145 and CRM-129a (Appendix A-6). To analyze the U isotopes, the instrument placed the sample uptake straw in a 50 ppb solution of the CRM-145 standard that had been spiked with the same amount of $^{233}U/^{236}U$ double-spike to achieve a ratio of U_{spike}/U_{sample} of ~1.7‰. The instrument was tuned to the maximum signal strength while up taking the CRM-145 solution starting with the sweep and sample gas, followed by the inlet system, source lens, and lastly, zoom optics. Once optimal tuning was achieved, a series of standards were run, with multiple iterations of the CRM-145

standard interspersed with the CRM-129a standard, which has a known isotopic offset with the CRM-145 standard of 1.7‰. Once the proper value of the CRM-129a standard bracketed with the CRM-145 standard had been measured at least five times, the sample analyses were able to proceed. The analytical session involved a CRM-145 standard run after every two samples with the isotopic composition of the samples calculated by bracketing with the CRM-145 standard ran before and after. After every ten samples, a CRM-129a standard was also run bracketed by two CRM-145 standards to ensure that the signal was still at the optimal strength and to account for any drift throughout the analytical session. In order to conduct replicate analyses, the analytical session spanned multiple days due to the nature of tuning the instrument to the proper specifications to ensure accurate measurements.

REE + Y preparation

Samples were prepared following the method in Tostevin et al. (2016) which is a multi-step leaching process. For best results, only samples with greater than 80 weight % carbonate were selected. Approximately 25 mg of sample powder was weighed out in a clean environment and placed in an individual 15 mL centrifuge tube. Once all samples had been weighed out accordingly, the samples were rinsed with milli-Q H_2O, agitated, then centrifuged for 10 minutes at 5000 rpm. The milli-Q water was discarded and the sequential leaching process was initiated. Each sample was spiked with 312.5 µL of 2% HNO_3 then agitated for approximately 20 minutes then left to leach overnight. The following morning each sample was centrifuged for 10 minutes at 5000 rpm and the solution was discarded. Each sample was then spiked with 625 µL of 2% HNO_3, agitated for approximately 20 minutes then left to leach overnight. The following morning, samples were centrifuged for 10 minutes at 5000 rpm and the solutions were decanted into fresh 15 mL centrifuge tubes. Solutions were then diluted up to 10 mL (+9.375 µL) with 2% HNO_3 and shipped off to Arizona State University where they await ICP-MS analysis.

A-2: Maps of the Siberian Craton

Figure 19: Map of the Siberian craton field region showing the location of the Patom/Ura Uplift, where the Chencha reef complex is located, and the Chernaya Rechka. The two formations are located roughly 2200 km away from each other.

Figure 20: Map of the Patom/Ura Uplift field area

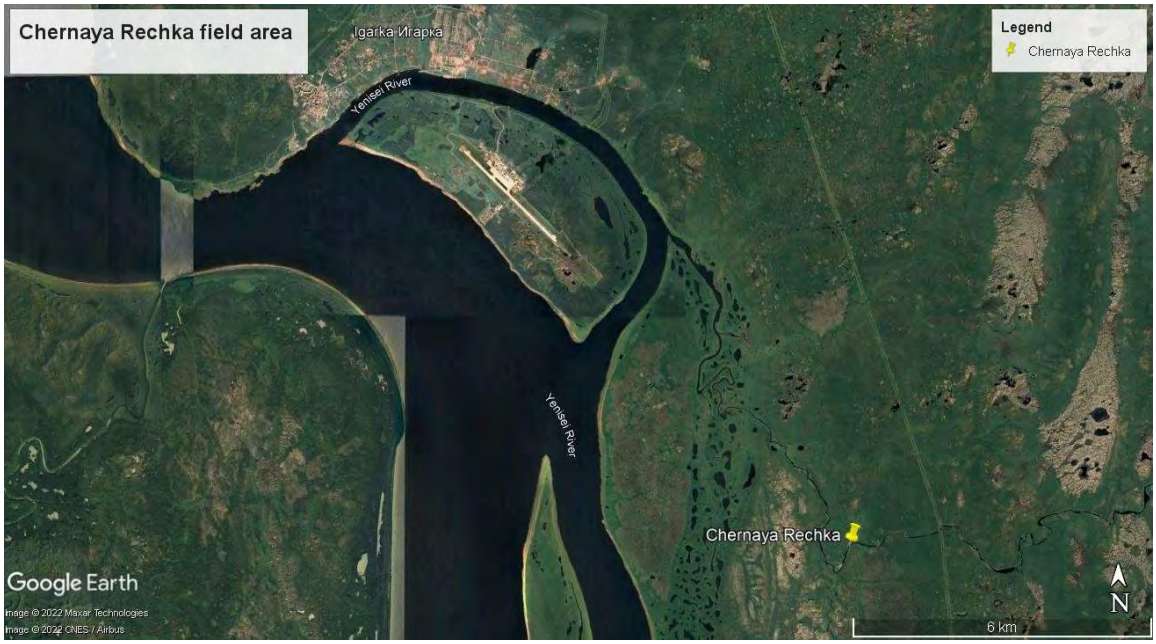

Figure 21: Map of the Chernaya Rechka field area.

A-3: Pb-Pb isochrons

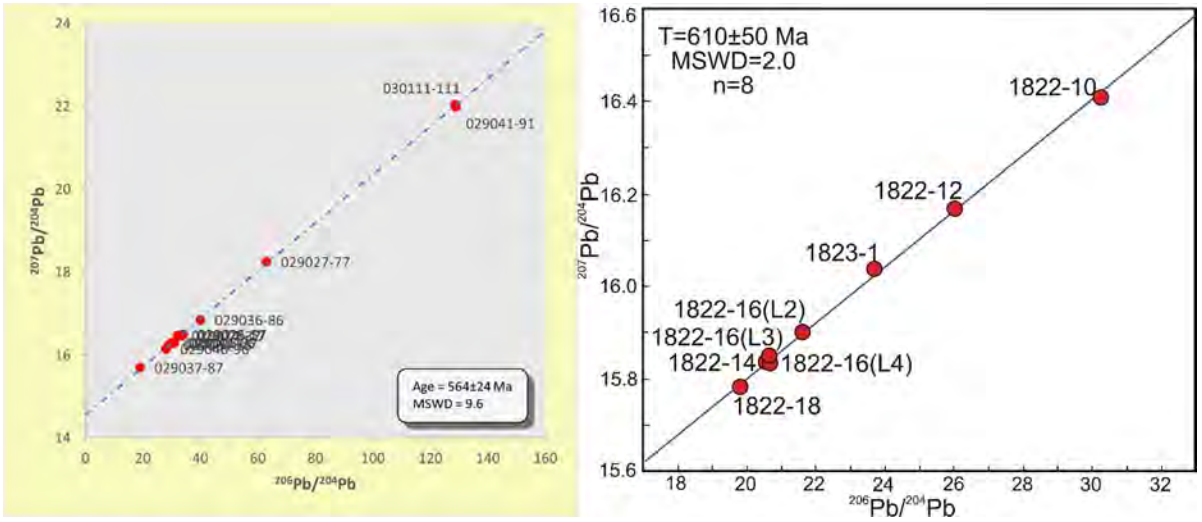

Figure 22: Pb-Pb isochron for the Chencha Formation on the left. The isochron constrains the age of the formation to 564 ± 24 Ma which overlaps with the Shuram Excursion (modified from image provided by Dmitriy Grazhdankin from Anton Kuznetsov 2022).

Pb-Pb isochron for the Chernaya Rechka Formation on the right. Current age constraints for the Chernaya Rechka Formation suggests it is 610 ± 50 Ma placing it between the late Cryogenian and the middle Ediacaran (Kochnev et al., 2022)

A-4: Element 2 ICP-MS

The Element 2 ICP-MS is a type of mass spectrometer that records elemental abundances in a liquid sample. Therefore, before undergoing any analysis, solid samples must be dissolved in acid (in the case of the [U] analysis it was a mixture of 35 mL 1M TMG HNO_3 and 5 mL concentrated TMG HNO_3). Samples are then poured into individual vials on a sample tray which is then loaded into the autosampler. Upon activation, a tube is inserted into the first sample and extracts the liquid in the sample vial then moves down the tray. The liquid is converted to an aerosol by a nebulizer which is then released into a plasma beam which ionizes the particles of different elemental composition. The ionized particles are then shot down a tube with a magnet that separates the particles based on mass and sends them down a mass-dependent path. Particles then travel through a hole in a small cone known as a Faraday collector which counts the number of times these particles hit the wall of the collector each second. The instrument then records the data and plots the counts per second against the known concentration of the standards used.

A-5: Correction algorithm for Element 2 ICP-MS

The Element 2 ICP-MS is a very precise instrument. However, it is not without flaw. As mentioned in S-5, there is a small hole in the Faraday collector which, over time, as more samples are ran, particles can get stuck in the hole preventing other particles from entering the collector. This ultimately leads to a decay of counts per second as the run progresses which throws the readings off. To account for this decrease the following correction algorithm is applied:

$$[U]correction = [U]\,raw\left(\frac{Sc\ sample\ 1\ cps}{Sc\ sample\ x}\right)$$

The [U] corrected value is calculated by taking the raw U concentration and multiplying it by the Sc counts/second in the first sample ran (the concentration of which is known) which is then divided by the Sc counts/second in the sample to be corrected. This equation gives values that account for the inevitable decay in sensitivity as samples are ran and it ensures that the concentration data gathered is consistent with the concentration of the samples.

A-6: Certified Reference Materials (CRM)

The purpose of using the certified reference materials in the Neptune Plus analysis is critical for ensuring accurate data. During analysis, it is possible for the Neptune to over count one mass over another which can change through time. A known solution is used to determine if this is occurring and if so, which mass is being over counted. CRM-145 is a common standard

for analyzing U isotopes and CRM-129a is often used as a quality control sample in conjunction with the CRM-145.

A-7: Agreement plots

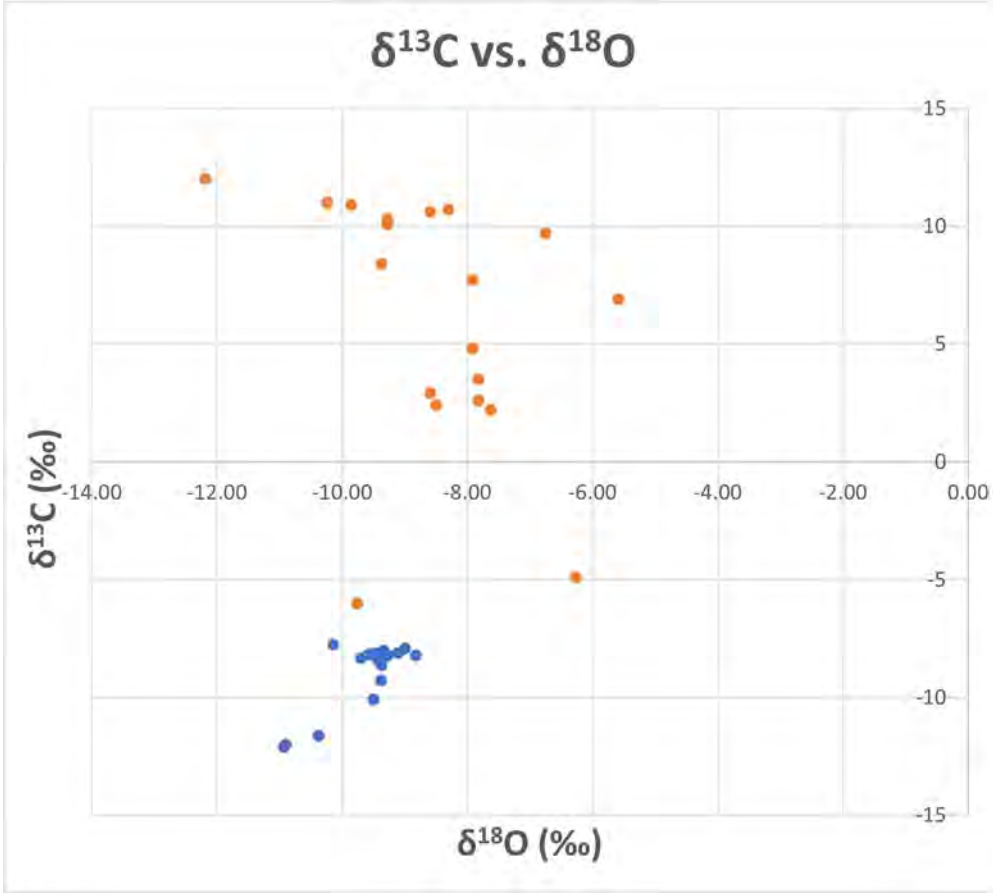

Figure 22: Plot displaying the agreement between the $\delta^{13}C$ and $\delta^{18}O$ values of the Chernaya Rechka Formation (orange) and Chencha Formation (blue). The $\delta^{13}C$ values in the Chernaya Rechka Formation displays a positive swing from -6‰ up to 12‰, while the $\delta^{13}C$ values from the Chencha Formaiton are fairly uniform within the -8‰ to -10‰ range. The $\delta^{18}O$ values in both formations do not show a significant variance in terms of values and are primarily within the -8‰ to -10‰ range. This lack of variance amongst the oxygen isotopes suggests the samples have not been significantly altered and have preserved their primary depositional composition.

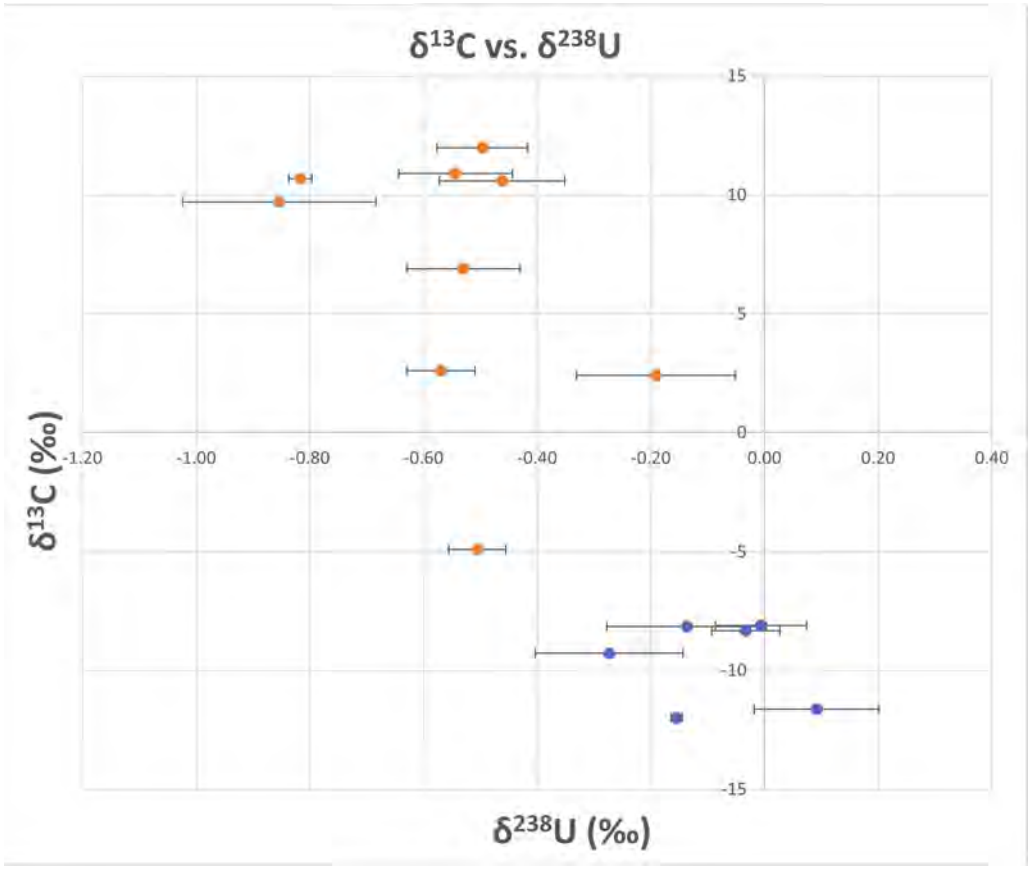

Figure 23: Plot displaying the agreement between the $\delta^{13}C$ and $\delta^{238}U$ values of the Chernaya Rechka Formation (orange) and Chencha Formation (blue). The carbon isotopic values in the Chernaya Rechka are more positive while the uranium isotopic values are more negative. The opposite is observed with the Chencha Formation carbon isotopic values which are more negative while the uranium isotopic values are more positive.

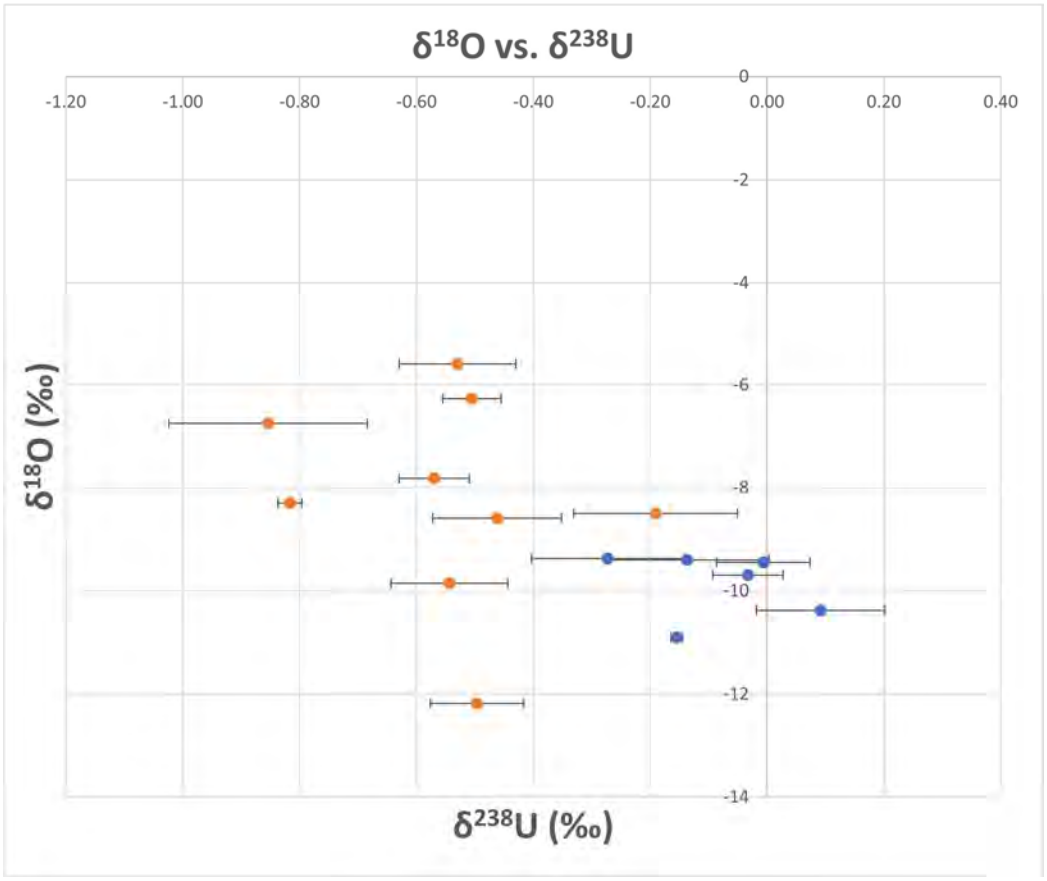

Figure 24: Plot displaying the agreement between the $\delta^{18}O$ and $\delta^{238}U$ values of the Chernaya Rechka Formation (orange) and Chencha Formation (blue). The uranium isotopic values are very different between the two formations with the Chernaya Rechka preserving more negative values while the Chencha preserves more positive values. However, the oxygen isotopic values are rather uniform with most falling between the -8‰ to -10‰ range.